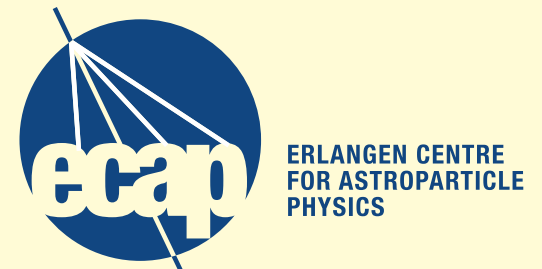
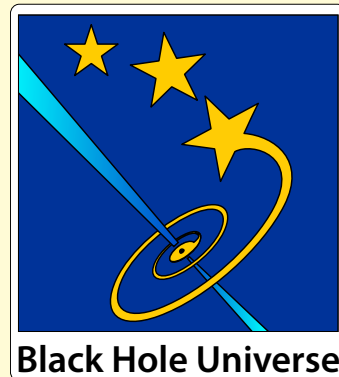


X-Ray Astronomy: Why and How

Emrah Kalemci
Sabancı Üniversitesi

Jörn Wilms
University of Erlangen-Nuremberg



Purpose of this lecture:

- Why do we do X-Ray Astronomy?
 - Accretion on Black Holes
 - Diagnostic Possibilities
- How do we do X-Ray Astronomy?
 - The need for Space
 - Balloons, Rockets, Satellites
 - Detection methods for X-rays and Gamma-rays

Literature

LONGAIR, M.S., 1992, *High Energy Astrophysics, Vol. 1: Particles, Photons, and their Detection*, Cambridge: Cambridge Univ. Press, ~50€

Good introduction to high energy astrophysics, the 1st volume deals extensively with high energy processes, the 2nd with stars and the Galaxy. The announced 3rd volume has never appeared. Unfortunately, everything is in SI units.

TRÜMPER, J., HASINGER, G. (eds.), 2007, *The Universe in X-rays*, Heidelberg: Springer, 96.25€

Recent book giving an overview of X-ray astronomy written by a group of experts (mainly) from Max Planck Institut für extraterrestrische Physik, the central institute in this area in Germany.

BRADT, H., 2004, *Astronomy Methods: A Physical Approach to Astronomical Observations*, Cambridge: Cambridge Univ. Press, \$50

Good general overview book on astronomical observations at all wavelengths.

Literature

CHARLES, P., SEWARD, F., 1995, *Exploring the X-ray Universe*, Cambridge: Cambridge Univ. Press, out of print

Summary of X-ray astronomy, roughly presenting the state of the early 1990s.

SCHLEGEL, E.M., 2002, *The restless universe*, Oxford: Oxford Univ. Press, 32€

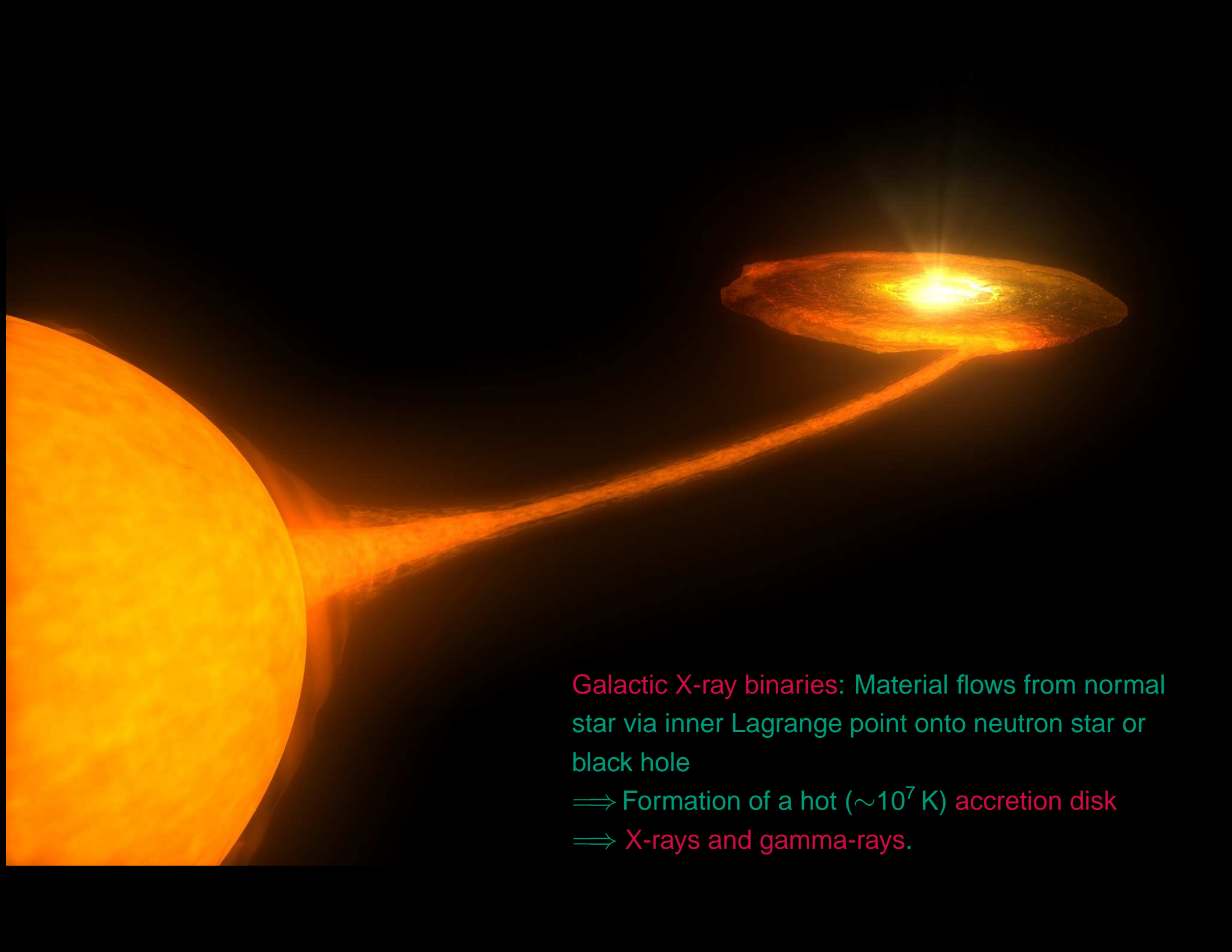
Popular X-ray astronomy book summarizing results from *XMM-Newton* and *Chandra*.

ASCHENBACH, B. et al., 1998, *The invisible sky*, New York: Copernicus

Popular “table top” book summarizing the results of the *ROSAT* satellite, with many beautiful pictures.

KNOLL, G.F., 2000, *Radiation Detection and Measurement*, 3rd edition, New York: Wiley, 126€

The bible on radiation detection. If you want one book on detectors, this is it.



Galactic X-ray binaries: Material flows from normal star via inner Lagrange point onto neutron star or black hole

⇒ Formation of a hot ($\sim 10^7$ K) accretion disk

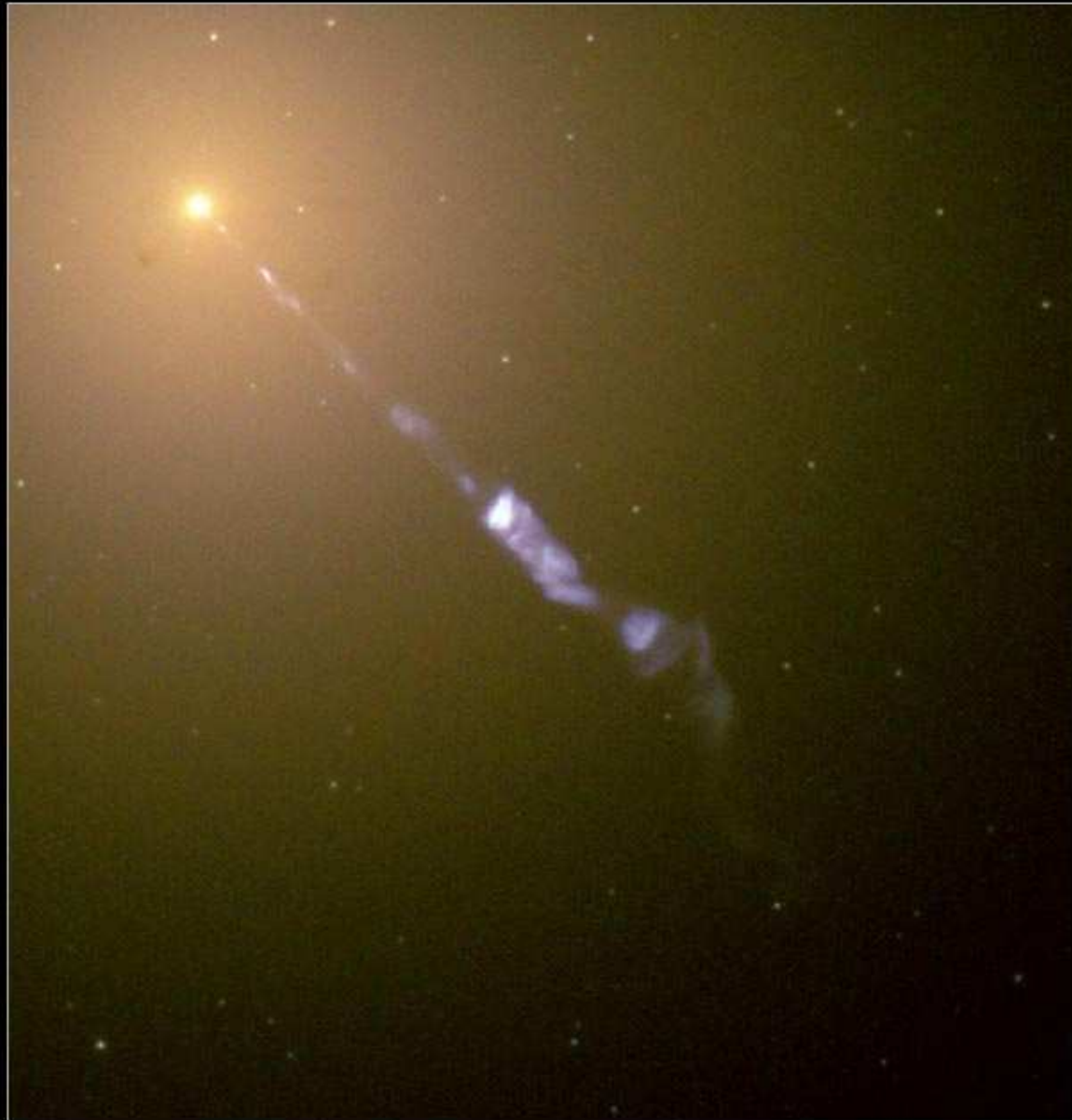
⇒ X-rays and gamma-rays.



M87: Image Credit & Copyright: Adam Block, Mt. Lemmon SkyCenter, U. Arizona

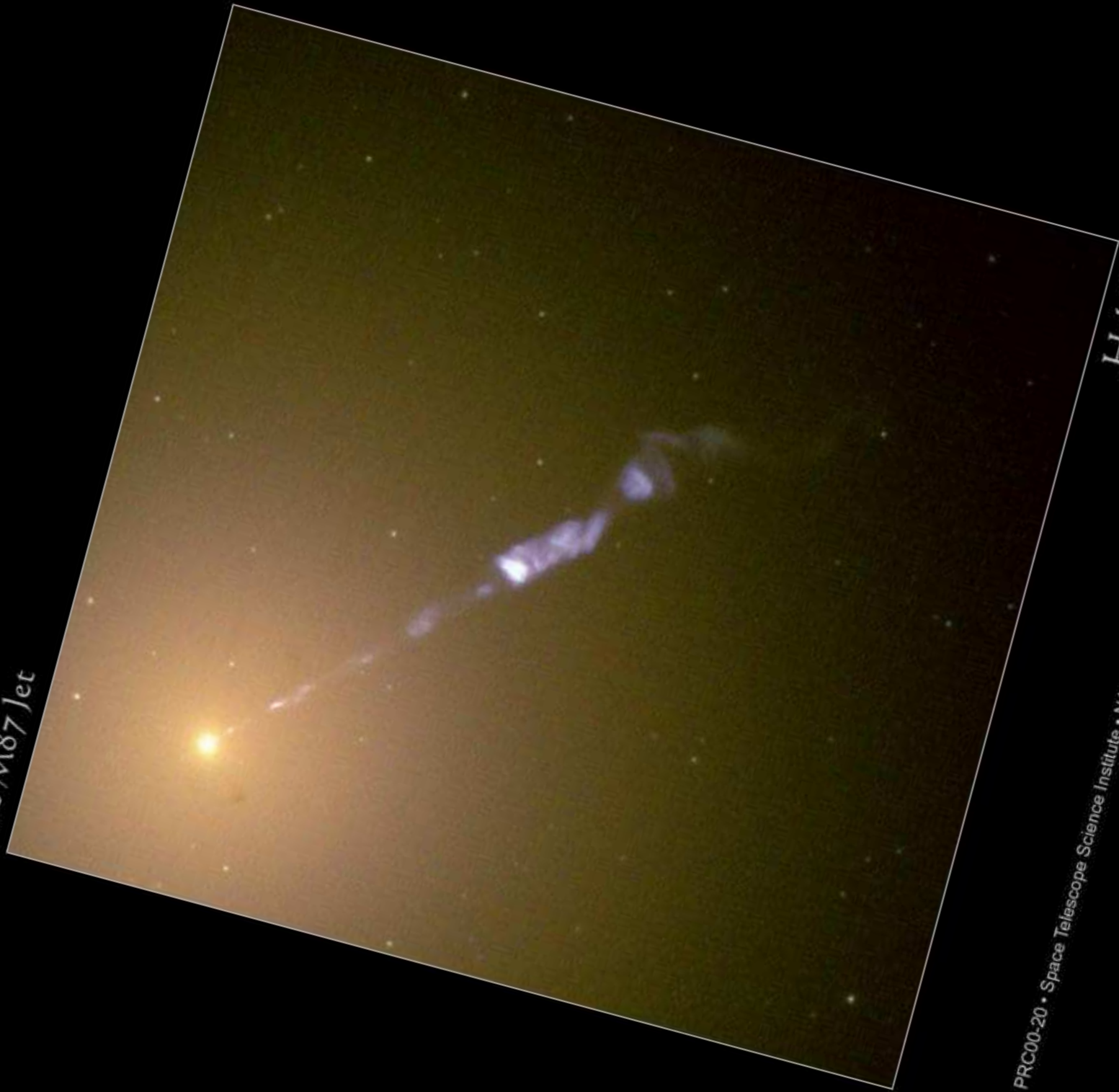
Extragalactic Black Holes

The M87 Jet



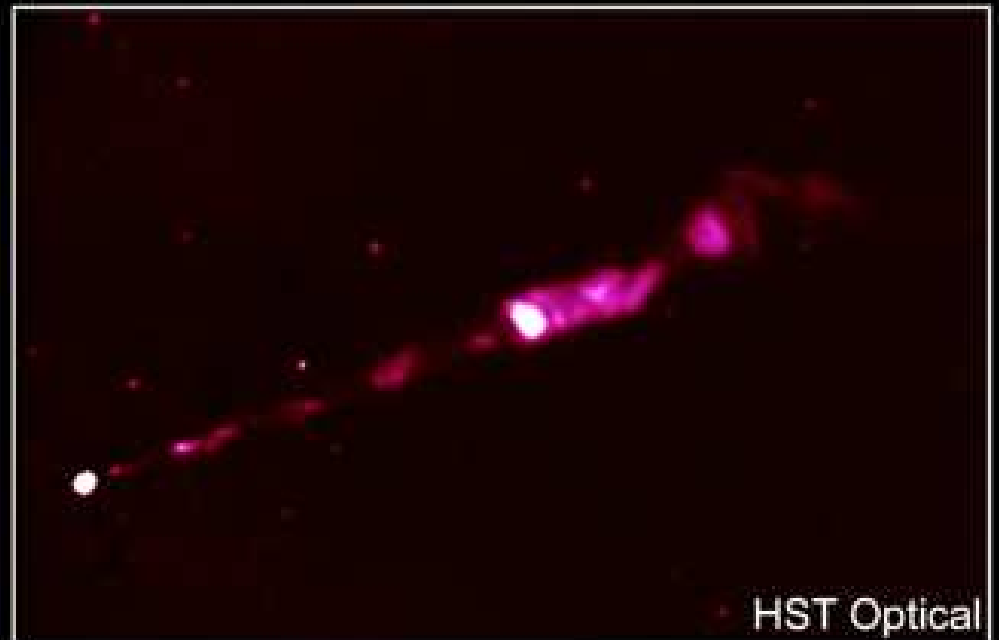
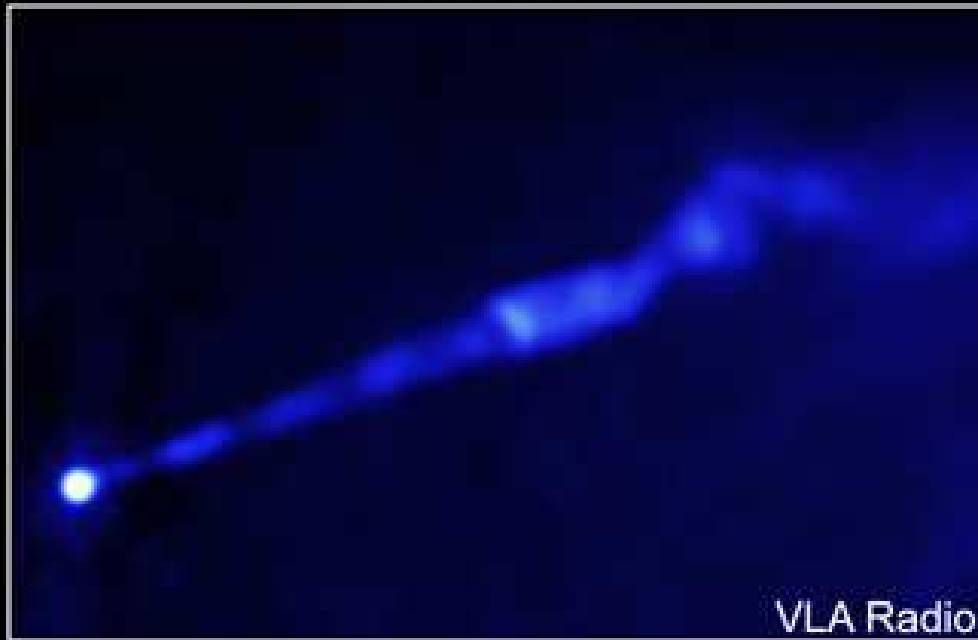
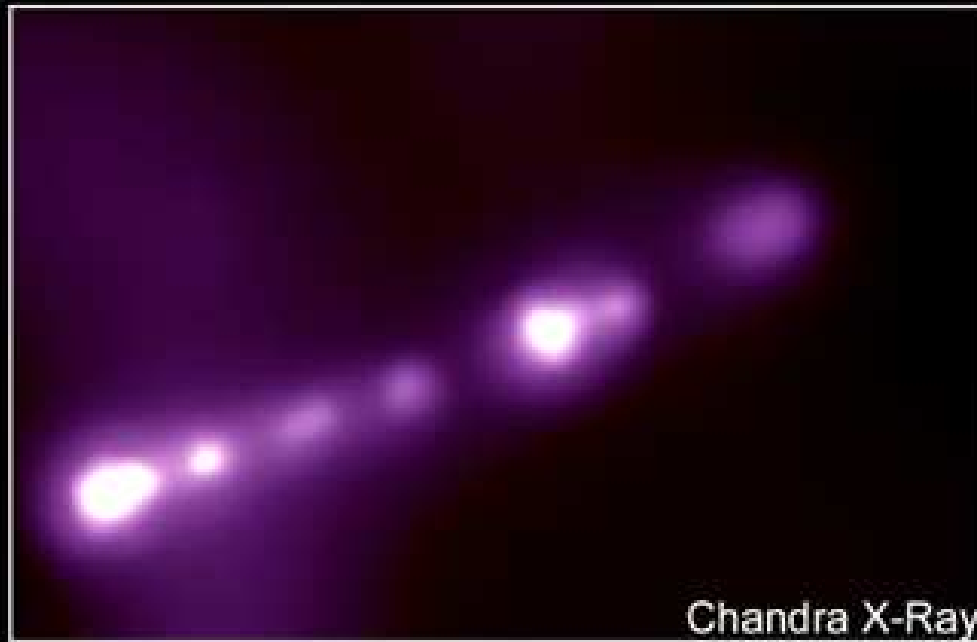
Hubble
Heritage

The M87 Jet



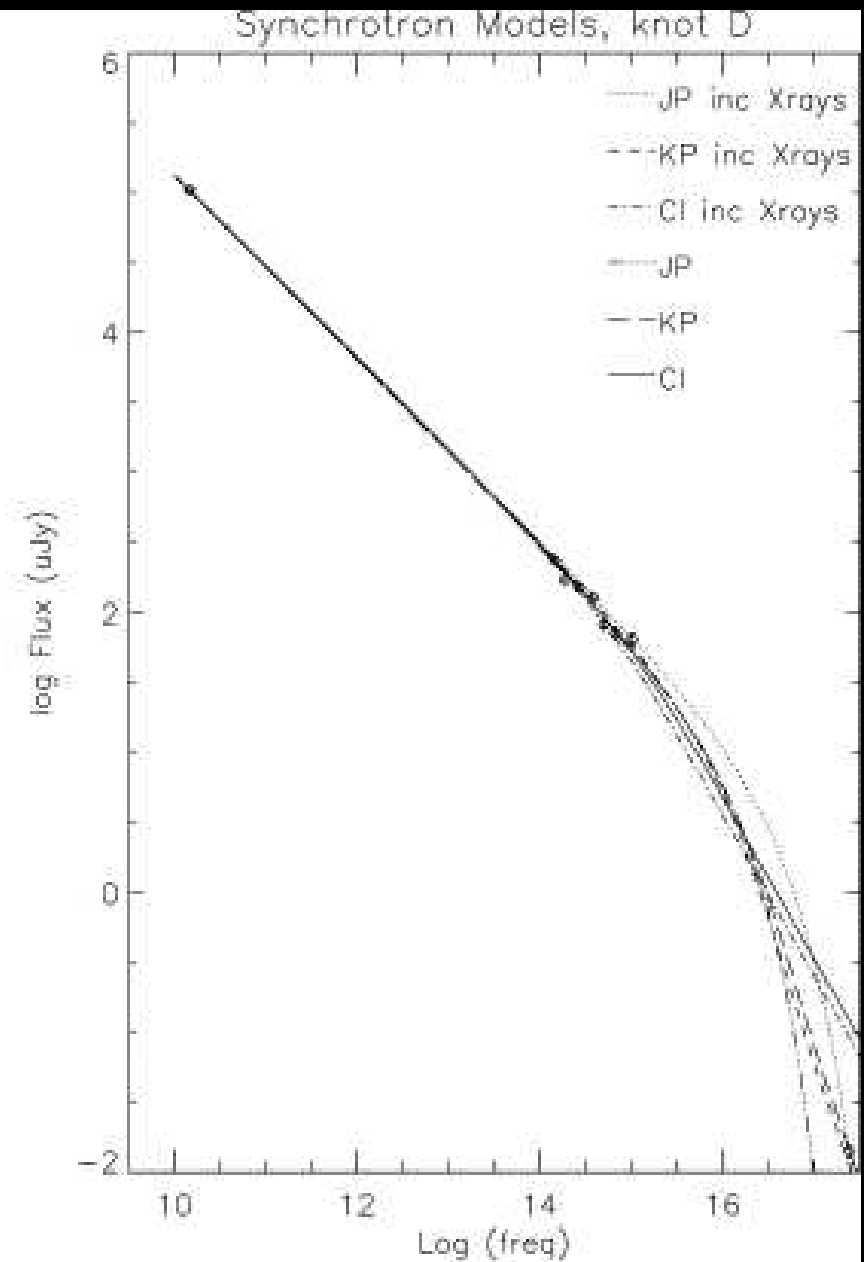
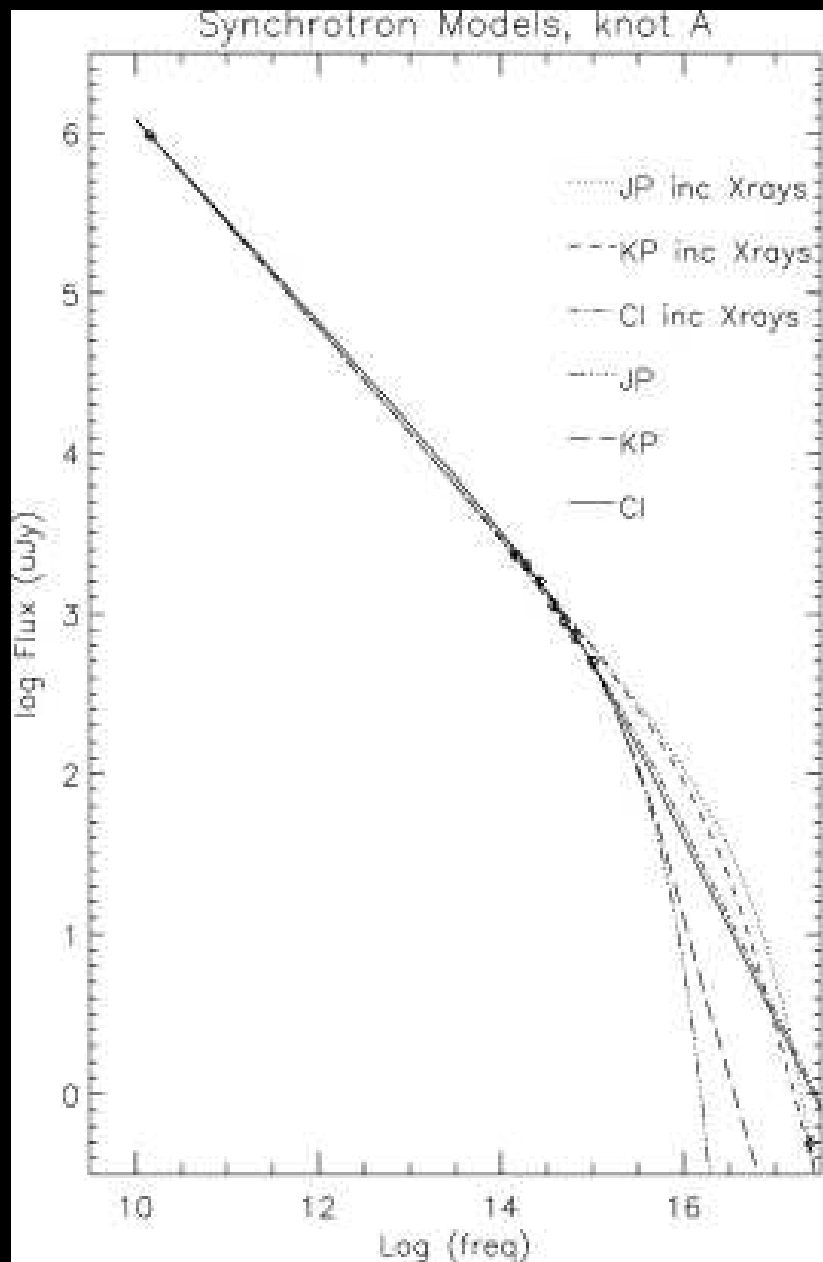
Hubble
Heritage

PRC00-20 • Space Telescope Science Institute • NASA and The Hubble Heritage Team (STScI/AURA)



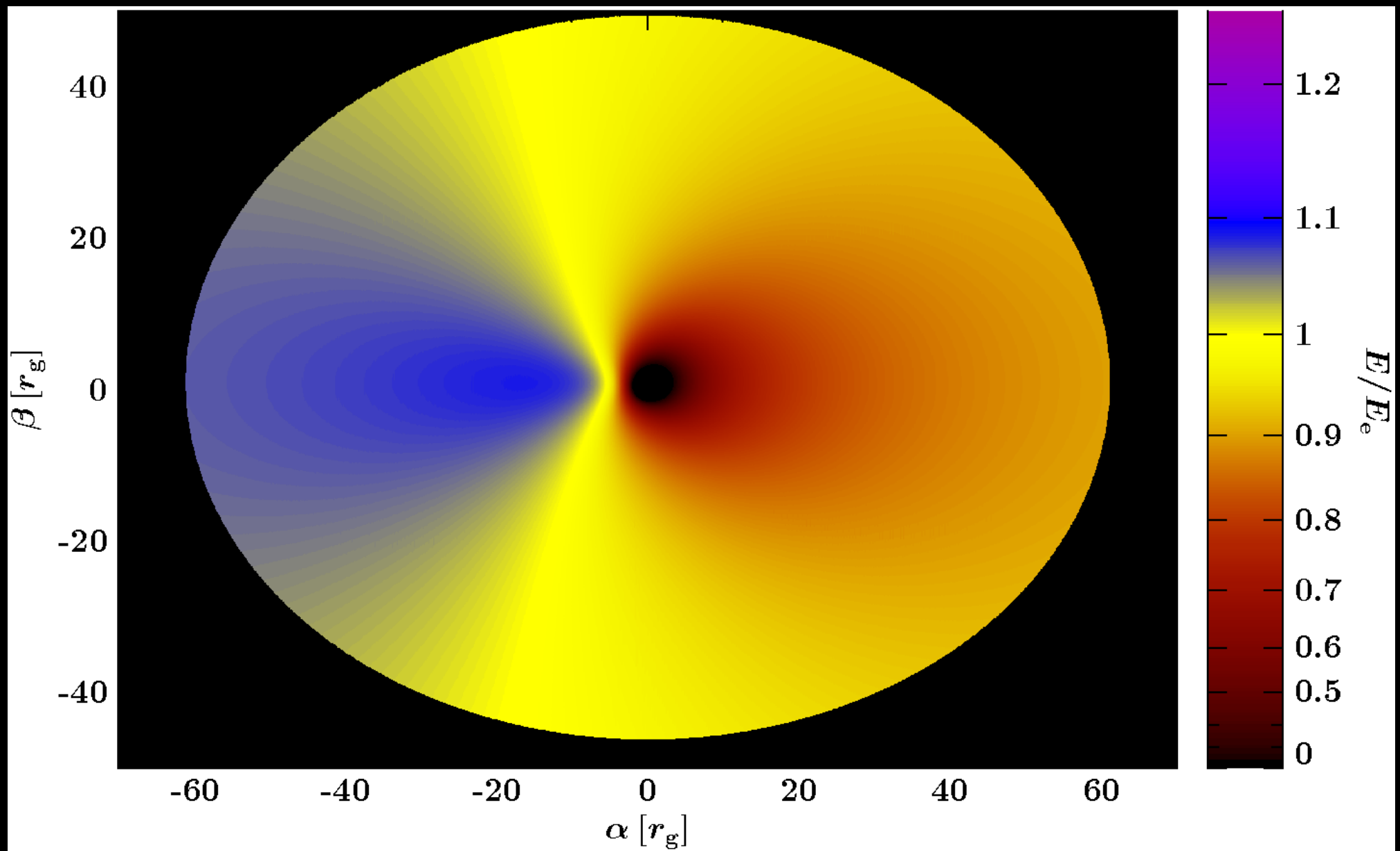
Credit: X-ray: NASA/CXC/MIT/H.Marshall et al. Radio: F.Zhou, F.Owen (NRAO), J.Biretta (STScI)

Optical: NASA/STScI/UMBC/E.Perlman et al.

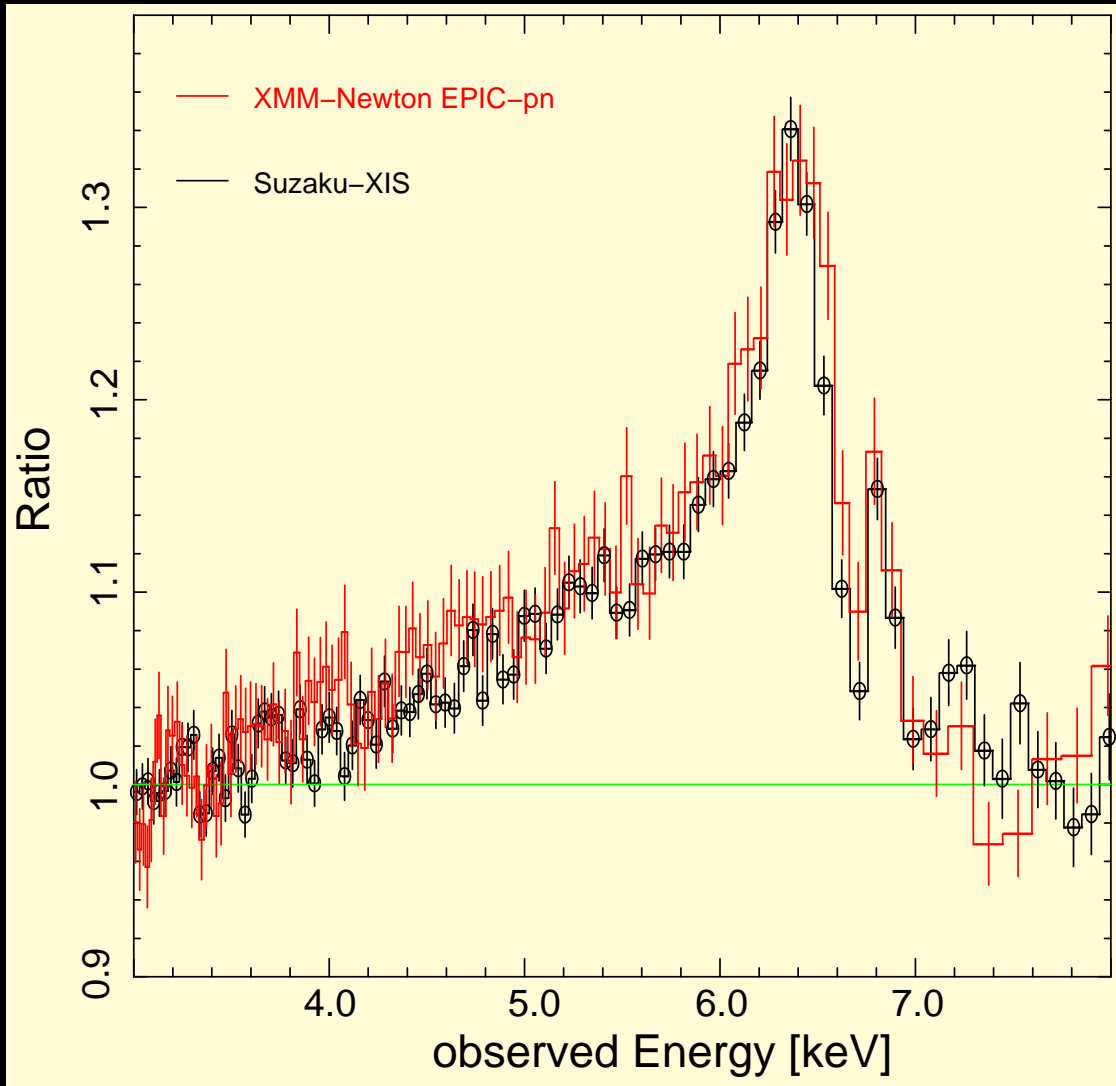


(M87; Perlman et al., 2002)

Many of the most extreme processes in the Universe produce broad band radiation.



Redshift distribution on an accretion disk (Dauser et al. 2010; submitted)



Emission lines from close to the black hole are strongly distorted by relativistic effects.

Measurement of the line shape allows determination of the parameters of the black hole and the accretion flow.

MCG-6-30-15

XMM-Newton and Suzaku (Miniutti et al., 2007)

IBIS coded mask

JEM-X coded mask

OMG

SPI

Instrument computers and electronics

IBIS detector

JEM-X detector

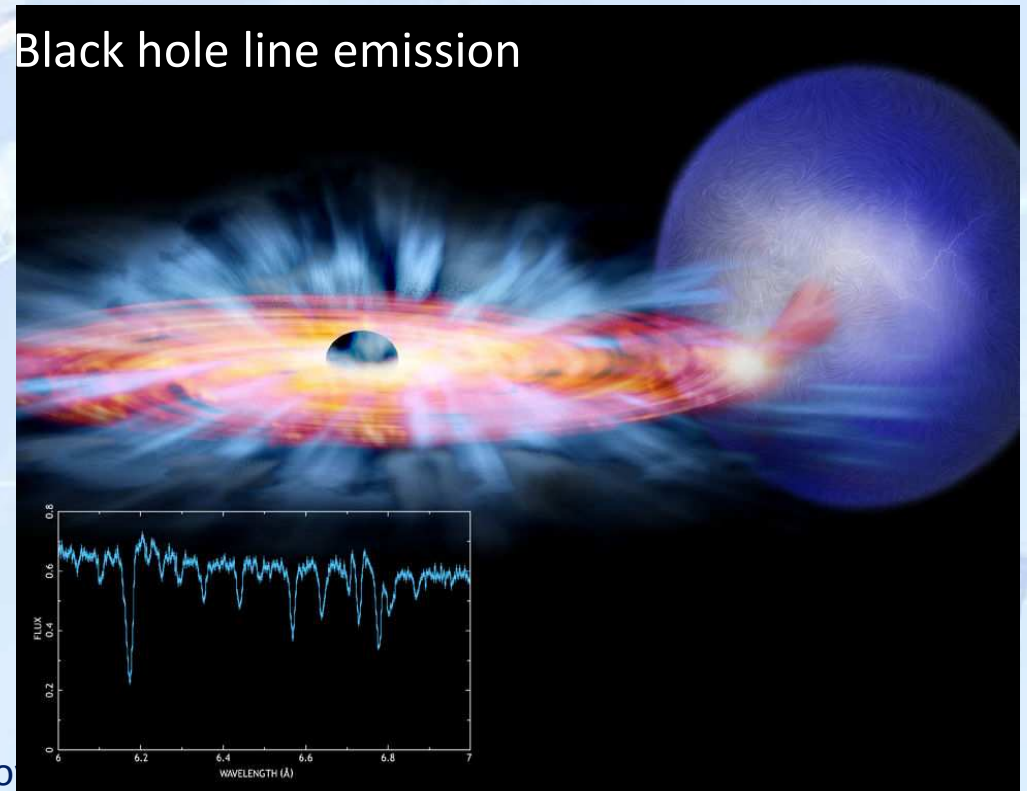
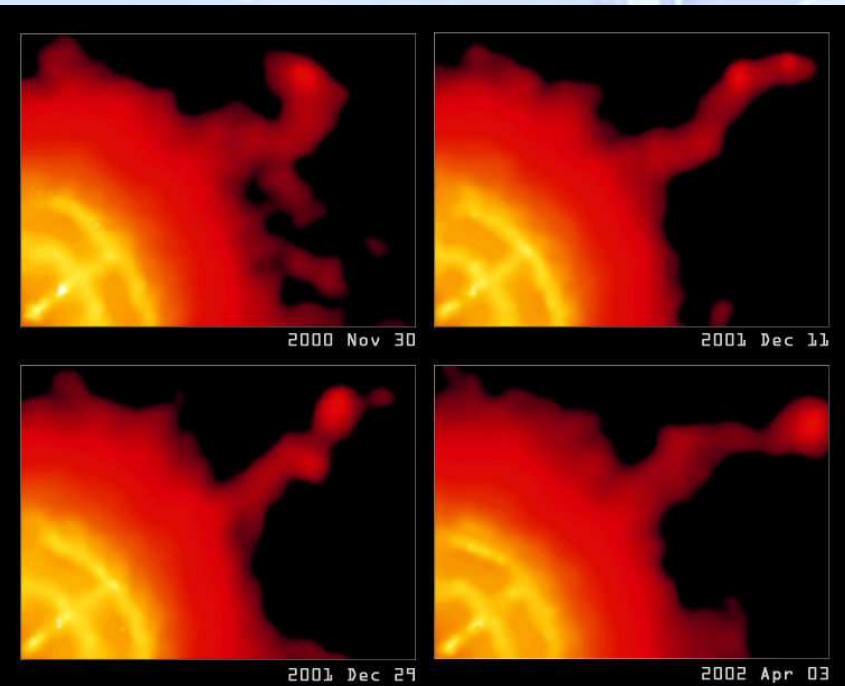
Power regulation

The astrophysical perspective

- X-rays (1keV - 200 keV): Energetic and penetrating (3 nm – 0.03 nm):
 - Stellar atmospheres, white dwarfs, neutron stars and black holes, active galactic nuclei, intra-cluster hot gas, jets, GRB afterglows.

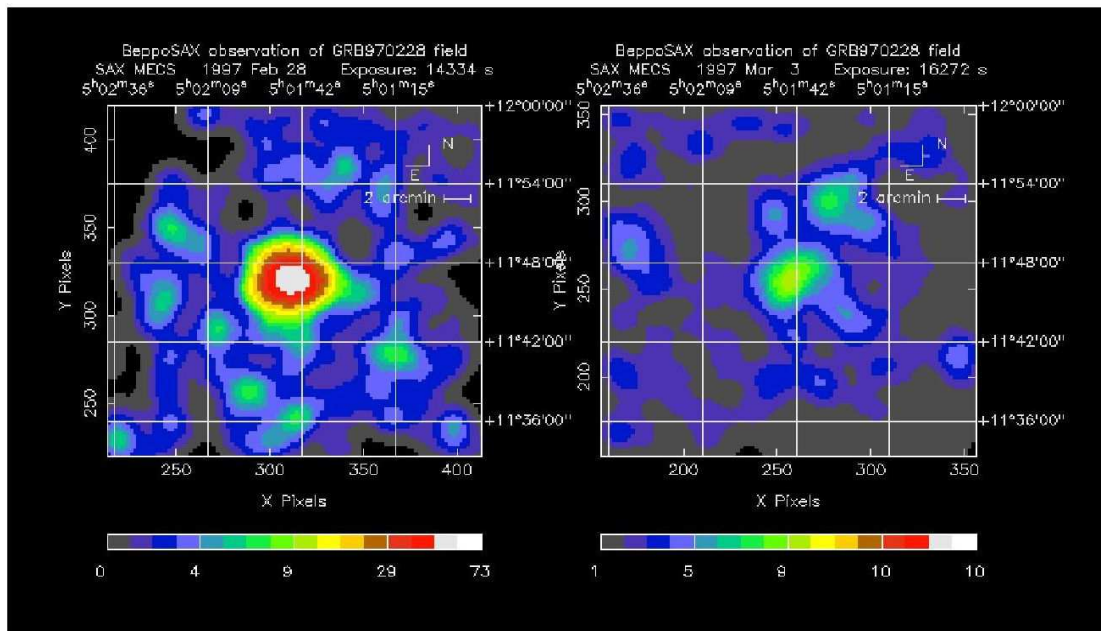
Vela powering its nebula and a jet

Black hole line emission

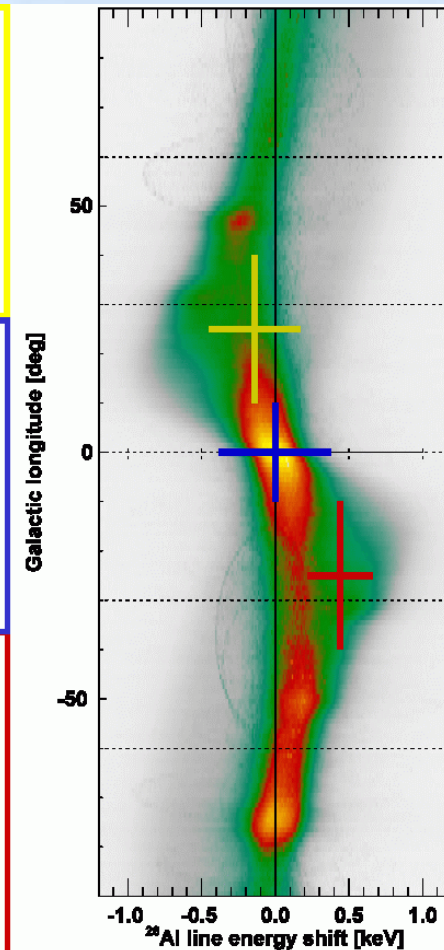
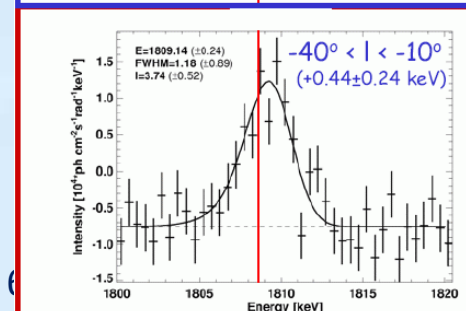
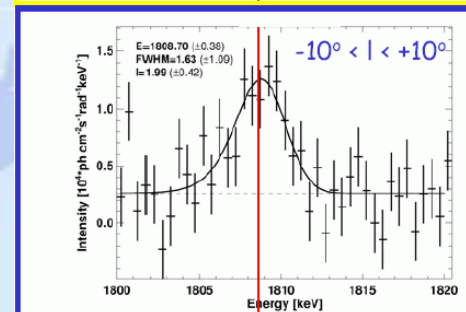
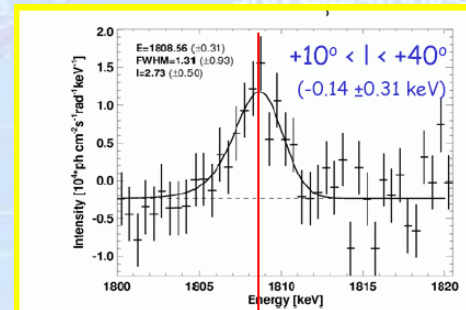


Why space astronomy, the astrophysical perspective

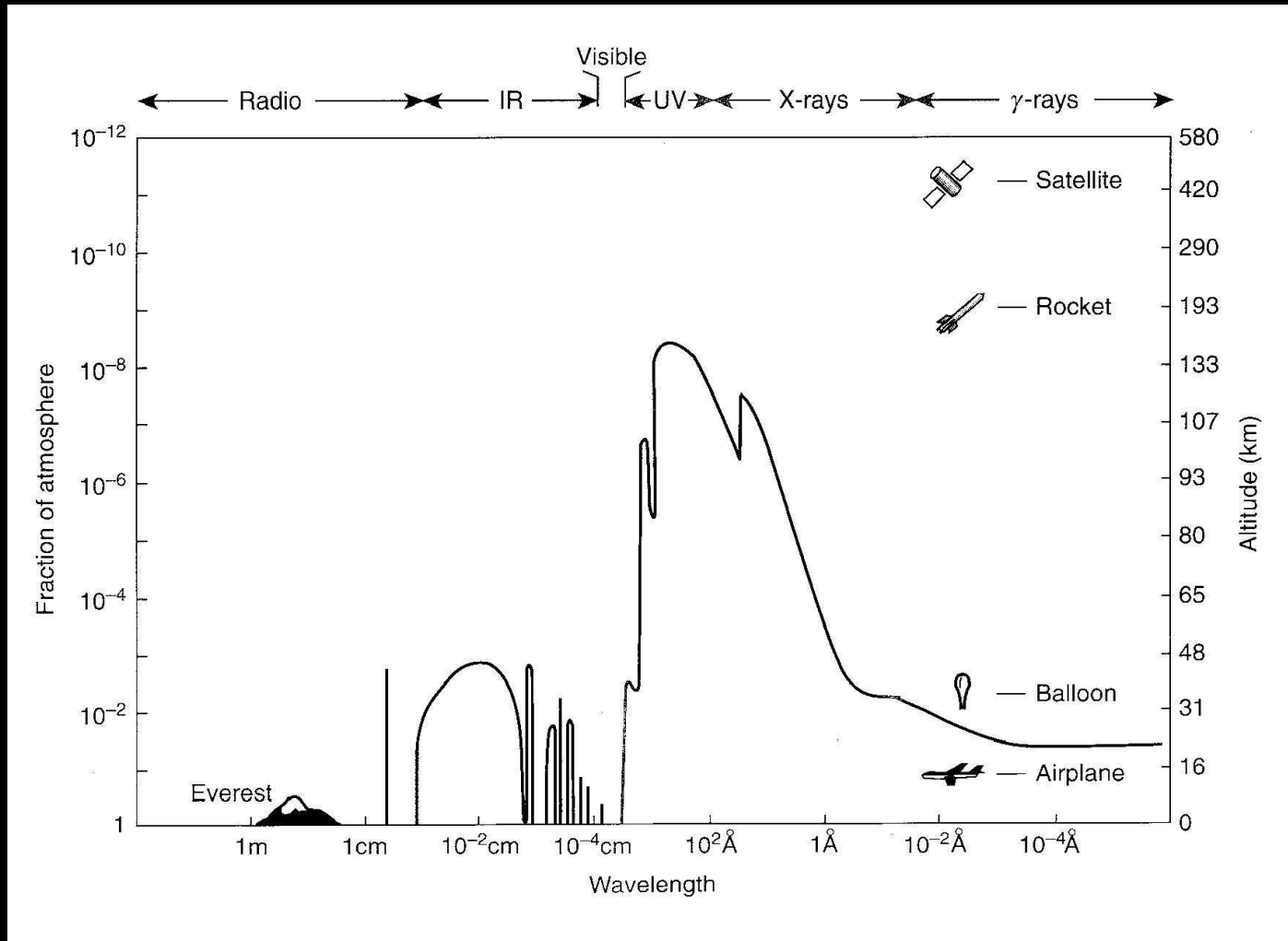
- Gamma-rays (> 200 keV):
 - Neutron stars, black holes, gamma-ray bursts, nucleosynthesis.



Beppo-Sax detection of the host galaxy of a GRB.



Part 2: Tools of the Trade: Satellites



Charles & Seward, Fig. 1.12

Earth's atmosphere is opaque for all types of EM radiation except for optical light and radio.

Major contributor at higher energies: photoabsorption ($\propto E^{-3}$), esp. from Oxygen (edge at ~ 500 eV).

⇒ If one wants to look at the sky in other wavebands, one *has* to go to space!

Ballooning:

(BIS coded mask)

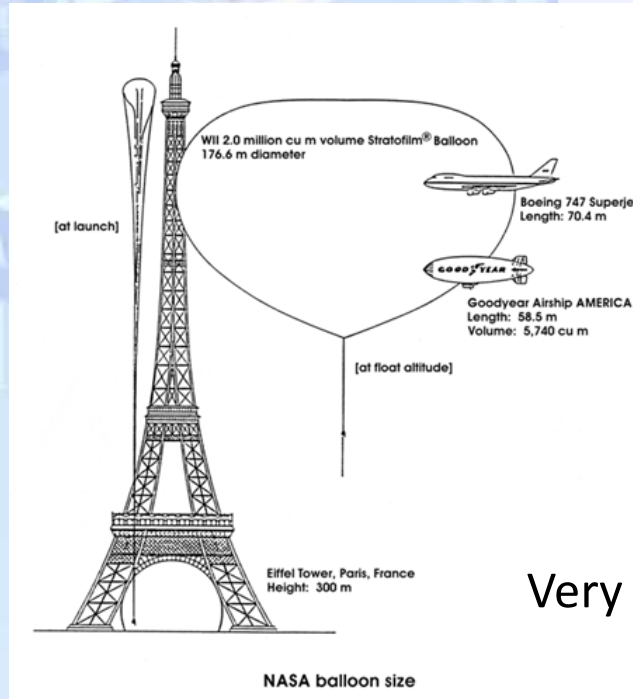
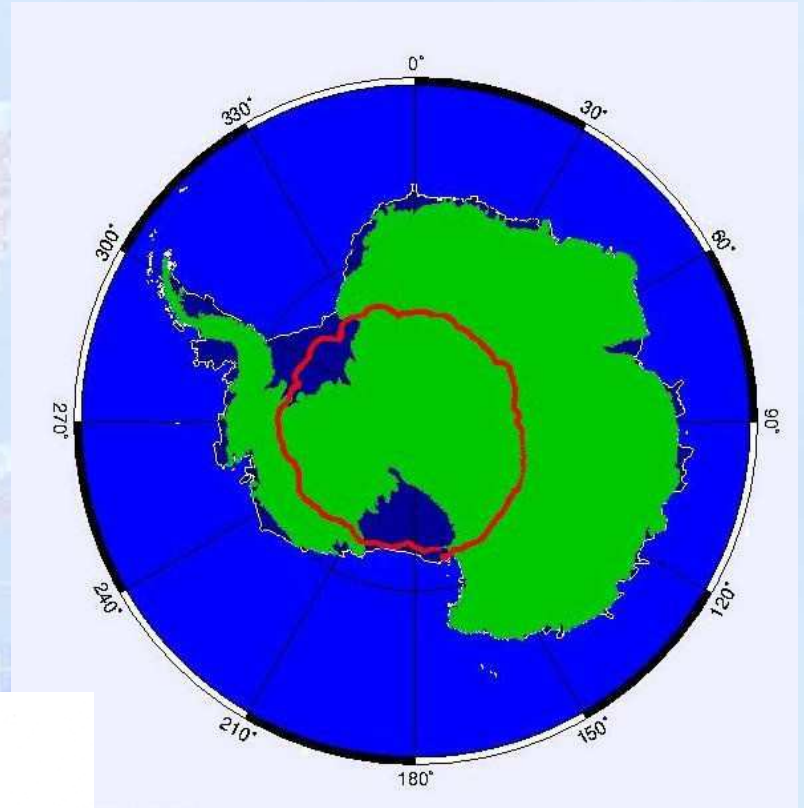


Climbs above 42 kms.

Uses stable winds

Very thin (0.002 cm) but strong material

Very large



Very difficult !

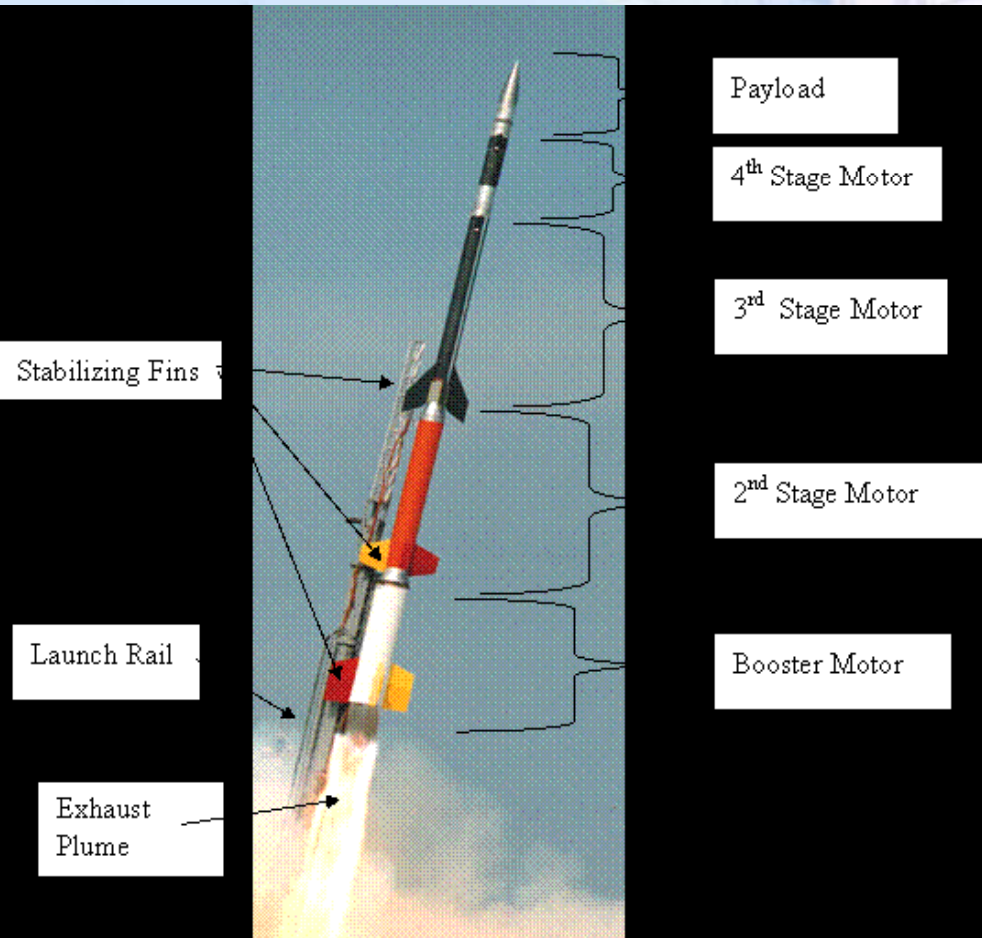


Sounding rockets:

Quick, low cost access to upper atmosphere with reusable (not always!) instruments. Rotates with a fixed period allowing pointed observations (without superb accuracy). Depending on weight, can go up to 1400kms and stays there for hundreds of seconds.

Payload module

Instrument computers and electronics



Payload module

IBIS coded mask

JEM-X coded mask

OMG

SPI

Instrument
and electronics

Even though rockets and balloons are mostly used for testing new Detector and telescope technologies, and testing equipment before a satellite launch, Especially rockets played a very important role in the birth and development of X-ray astronomy in 1960s and 1970s! R. Giacconi got the Nobel Prize for the Pioneering work (including discovery of Sco X-1, the brightest X-ray source in the sky.



Instrument computers
and electronics

Detector bench

Attitude control
electronics

Batteries

Fuel tanks

Attitude sensors

Solar panels

Courtesy of Rick Rothschild.

SATELLITES

Payload module

IBIS coded mask

JEM-X coded mask

OMC

SPI

Instrument computers and electronics

IBIS detector

JEM-X detectors

Power regulation

Reaction wheels for pointing the spacecraft

Data handling and telecommunication

Service module

Star trackers

Instrument computers and electronics

Detector bench

Attitude control electronics

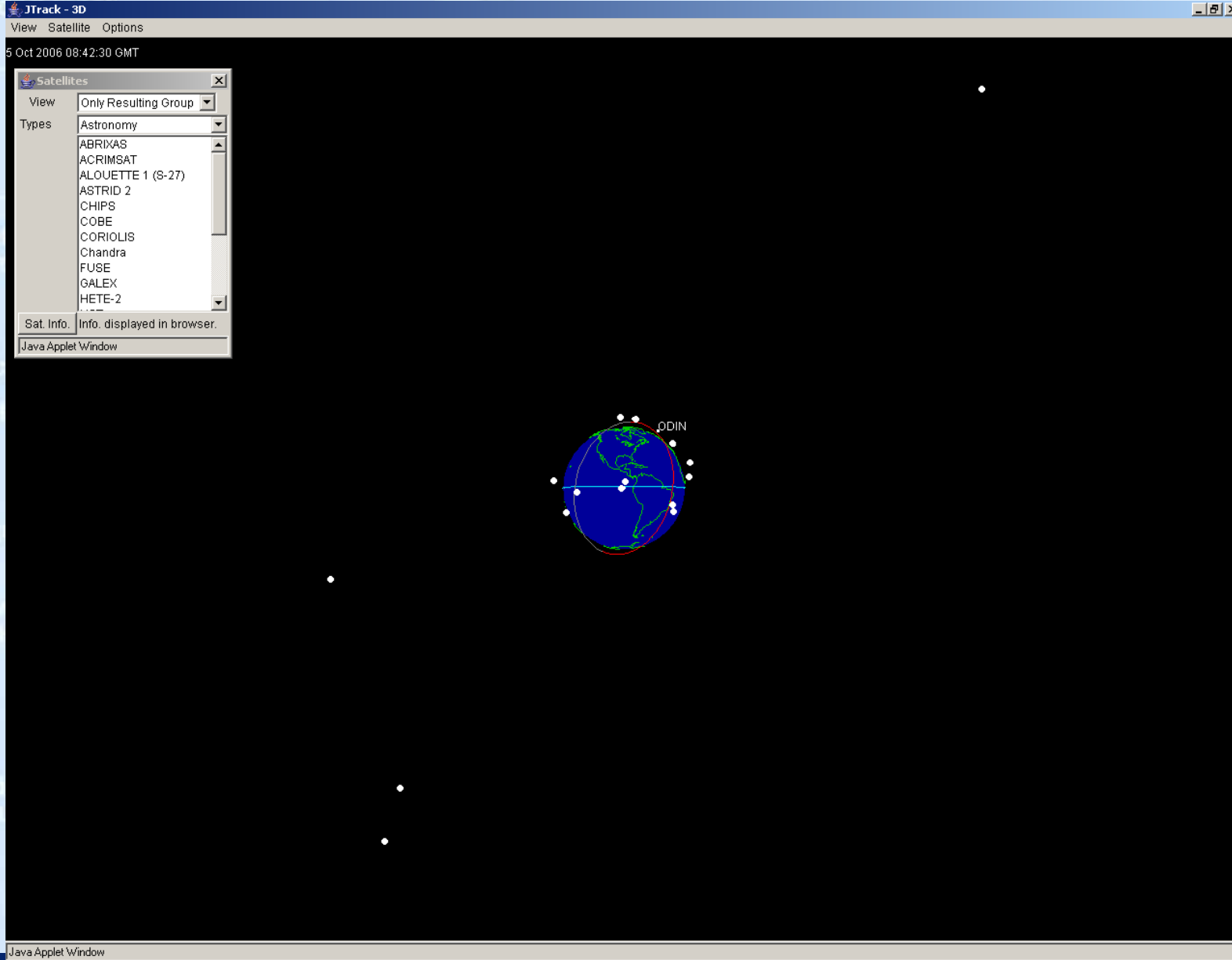
Batteries

Fuel tanks

Attitude sensors

solar panels

Where are astronomy satellites?



ORBITS

IBIS coded mask

JEM-X coded mask

OMG

SPI

Instrument control and electronics

IBIS detector

JEM-X detector

Power regulation

Reaction point

Data transfer

JTrack - 3D
View Satellite Options
5 Oct 2006 08:19:46 GMT

Satellites
View: All
Types: Physics
ATS 1
ATS 3
CRRES
ERBS
FAST
GMS 5
GOES 7
GOES 8
GOES 9
INTEGRAL
INTERCOSMOS 24

Sat. Info. Info. displayed in browser.
Java Applet Window

INTEGRAL

Highly eccentric orbits, scientific only.

Java Applet Window

Why low earth orbit?

Two harmful radiation belts exist: at ~3000 km (5000 km thick) and at 16000 km (~7000 km thick). **Below 1000 km is ok for satellites.**

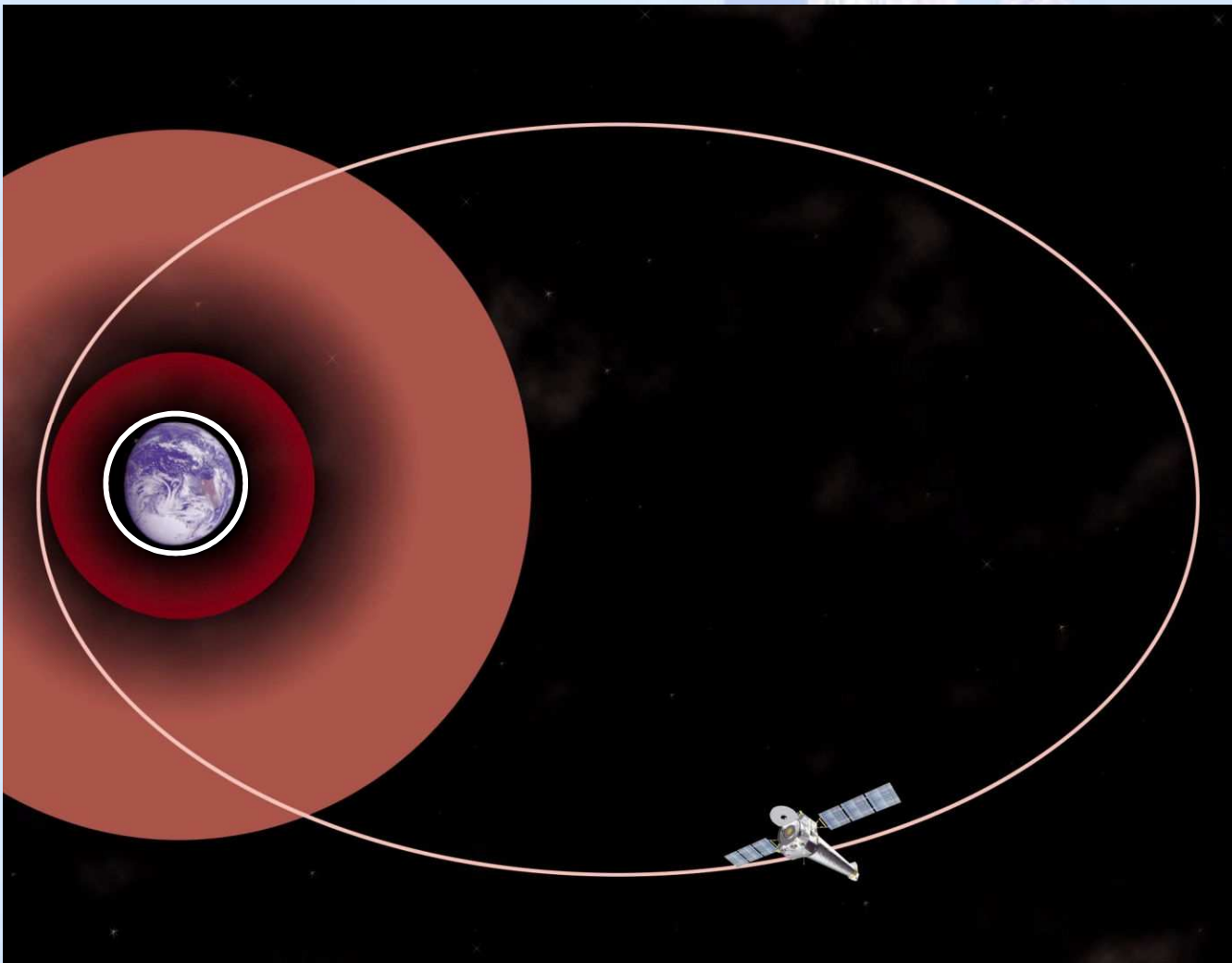
2 problems with radiation belts: Within the belts very high background, energetic particles affect semiconductor detectors, and degrades electronic circuits.

Above the belts, cosmic ray background high.
Easy for maneuvering, cheap and easy to place into orbit (one phase launch)

Why not low earth orbit

- Large eclipses due to earth. Impossible for continuous coverage (Efficiency 65-70%).

Eccentric orbits:



- Much better efficiency and coverage.
- Higher overall background
- Higher exposure to radiation belts
- 2 stage launch.
Expensive

Special orbits

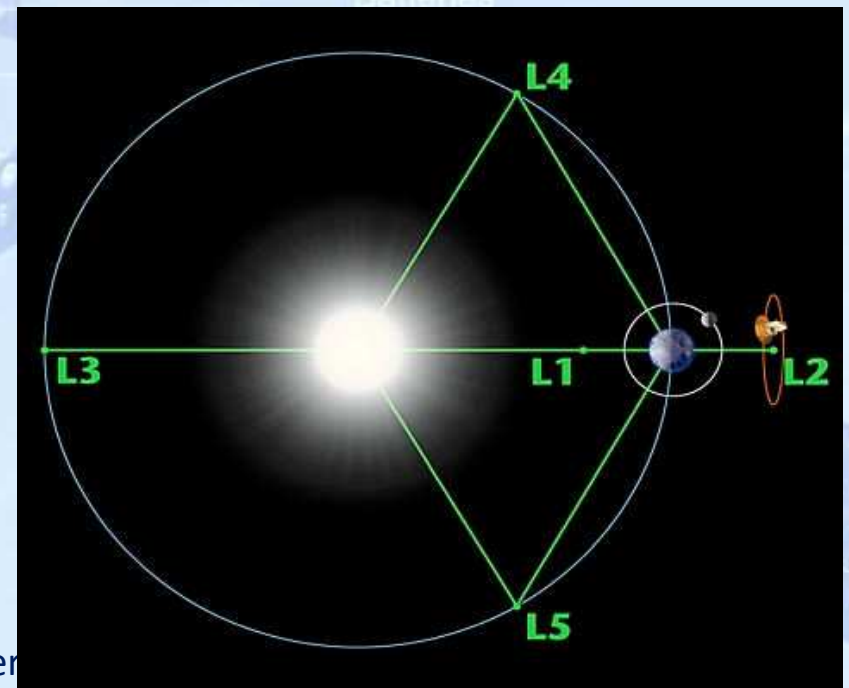
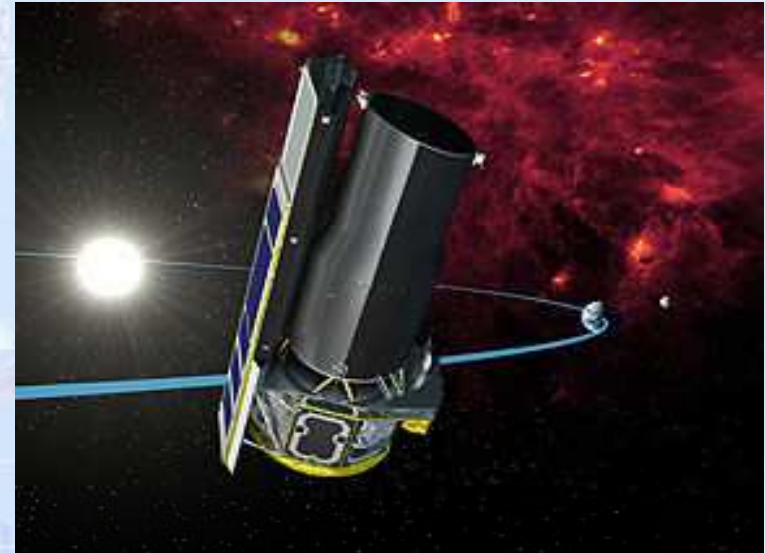
- **Trailer:**

Trails earth. Stays cool, require much less liquid Helium.

Separates 0.1 AU/year.

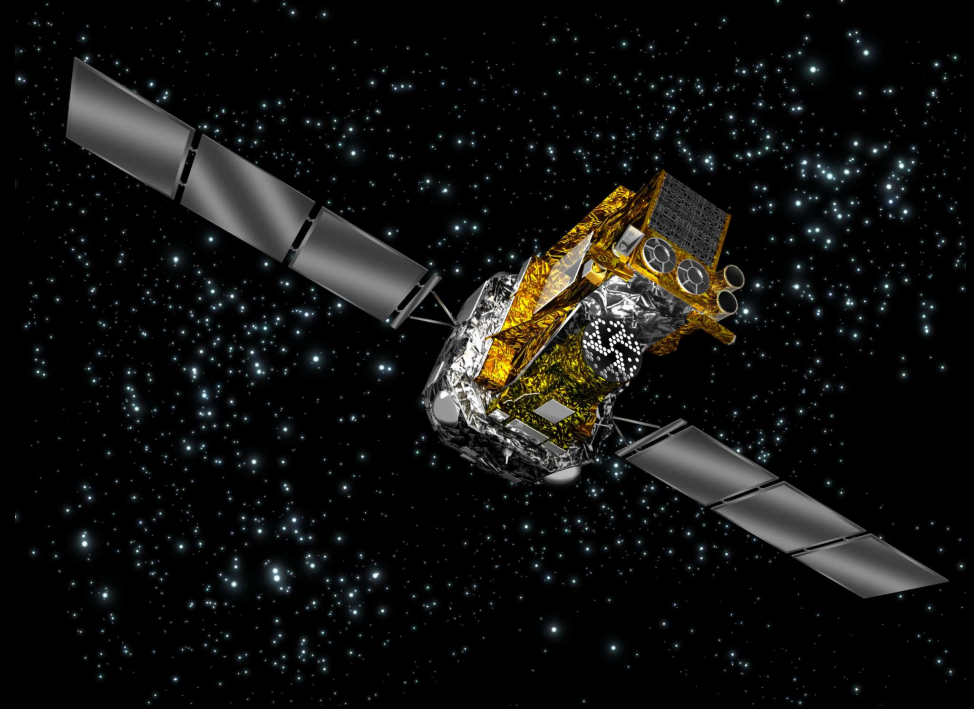
- **Lagrange point**

Stays at unstable lagrange points L1 (like sun observing SOHO) or L2 (like WMAP). Need adjustments every 20 days- no radiation belt, 100% efficiency.





XMM-Newton (ESA): launched 10 Dec. 1999



INTEGRAL (ESA): launched 17 Oct 2002

Currently active missions: *X-ray Multiple-Mirror Mission (XMM-Newton; ESA)*, *Chandra (USA)*, *International Gamma-Ray Laboratory (INTEGRAL; ESA)*, *Swift (USA)*, *Rossi X-ray Timing Explorer (RXTE) (USA)*, *High Energy Transient Explorer (HETE-2; USA)*, *Fermi (aka GLAST; USA)*, *High Energy Solar Spectroscopic Imager Spacecraft (RHESSI; USA)*, *Suzaku (Japan, USA)*, *AGILE (Italy)*.

Planned missions: *ASTROSAT (India)*, *Spectrum-X-Gamma (Russia/Germany/France)*, *Astro-H (Japan/USA)*, *NuSTAR (USA)*, *GEMS (USA)*, *IXO (USA/ESA/Japan)*

We're living in the "golden age" of X-ray and gamma-ray astronomy.

IBIS coded mask

JEM-X coded mask

OMG

X-ray Telescopes

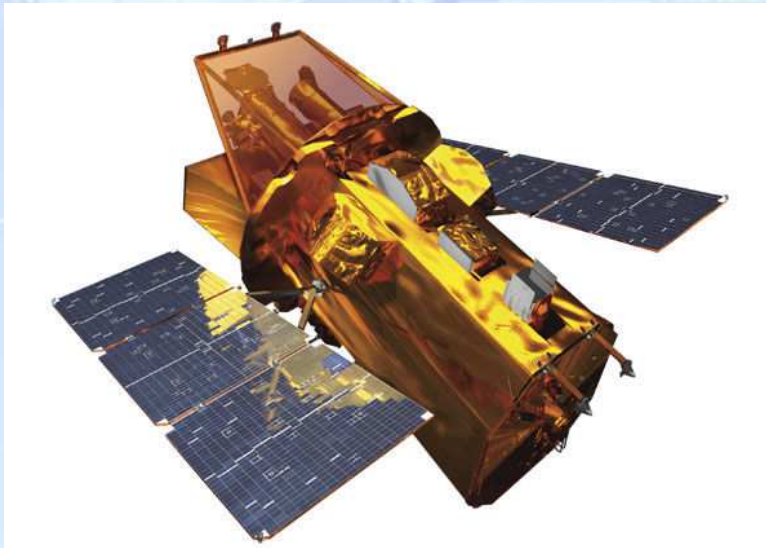


Chandra – superb angular resolution, energy resolution.

Data handling and telecommunication



XMM-Newton, large collecting area.



Swift, fast response!

Part 3: Tools of the Trade: Detectors

Introduction

There are two steps in the X-ray detection process:

1. Collection of X-rays (“imaging”)

- **Wolter telescopes** (soft X-rays up to ~ 15 keV)
- **Coded Mask telescopes** (above that)

Or just use a collimator

2. Detection of X-rays

- **Non-imaging detectors**

Detectors capable of detecting photons from a source, but without any spatial resolution

⇒ Require, e.g., **collimators to limit field of view** or use these to form individual pixels.

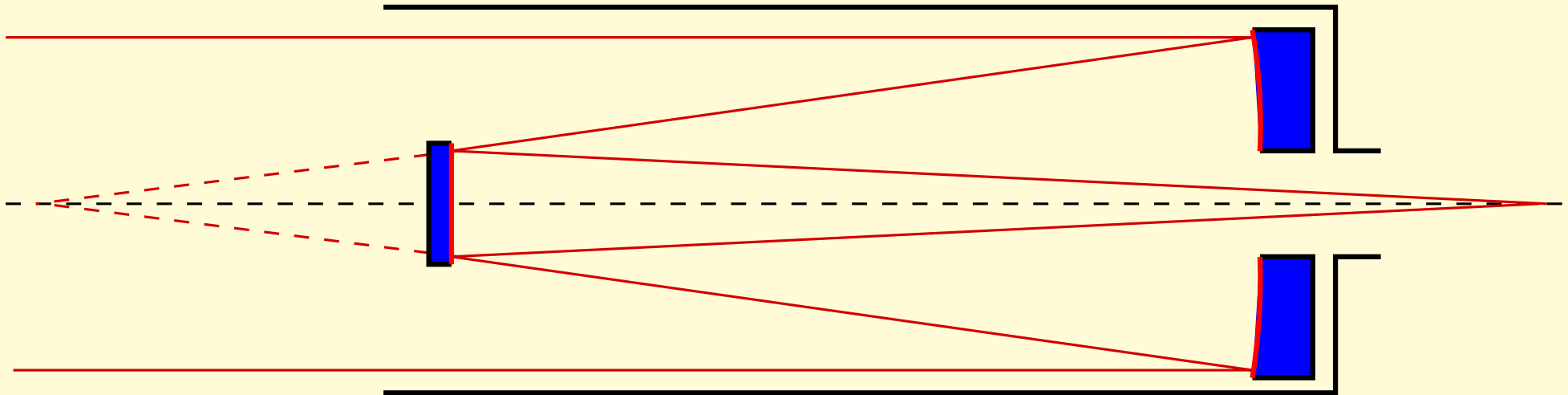
Example: **Proportional Counters, Scintillators**

- **Imaging detectors**

Detectors with a spatial resolution, typically used in the IR, optical, UV or for soft X-rays. **Generally behind some type of focusing optics.**

Example: **Charge coupled devices (CCDs), Position Sensitive Proportional Counters**

Imaging



Cassegrain telescope, after Wikipedia

Reminder: Optical or radio telescopes are usually reflectors:

primary mirror → secondary mirror → detector

Main characteristics of a telescope:

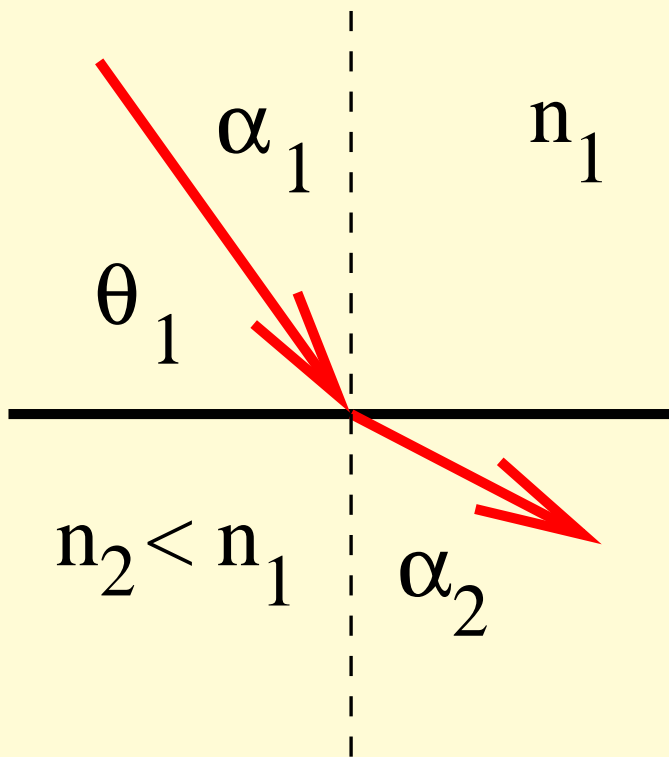
- collecting area (i.e., open area of telescope, $\sim \pi d^2/4$, where d : telescope diameter)
- for small telescopes: angular resolution,

$$\theta = 1.22 \frac{\lambda}{d} \quad (1)$$

but do not forget the seeing!

Imaging

Optical telescopes are based on principle that reflection “just works” with metallic surfaces. For X-rays, things are more complicated. . .



Snell's law of refraction:

$$\frac{\sin \alpha_1}{\sin \alpha_2} = \frac{n_2}{n_1} = n \quad (2)$$

where n index of refraction, and $\alpha_{1,2}$ angle wrt. surface normal. If $n \gg 1$: **Total internal reflection**

Total reflection occurs for $\alpha_2 = 90^\circ$, i.e. for

$$\sin \alpha_{1,c} = n \iff \cos \theta_c = n \quad (3)$$

with the critical angle $\theta_c = \pi/2 - \alpha_{1,c}$.

Clearly, total reflection is only possible for $n < 1$

Light in glass at glass/air interface: $n = 1/1.6 \implies \theta_c \sim 50^\circ \implies$ principle behind **optical fibers**.

Imaging

In general, the index of refraction is given by the **Maxwell relation**,

$$n = \sqrt{\epsilon\mu} \quad (4)$$

where ϵ : dielectricity constant, $\mu \sim 1$: permeability of the material.

For **free electrons** (e.g., in a metal), Jackson (1975, eq. 7.59) shows that

$$\epsilon = 1 - \left(\frac{\omega_p}{\omega}\right)^2 \quad \text{with} \quad \omega_p^2 = \frac{4\pi n Z e^2}{m_e} \quad (5)$$

where ω_p is called the **plasma frequency** and where n is the number density of atoms and Z is the nuclear charge.

(i.e., nZ is the number density of electrons)

With $\omega = 2\pi\nu = 2\pi c/\lambda$, Eq. (5) becomes

$$\epsilon = 1 - \frac{n Z e^2}{\pi m_e c^2} \lambda^2 = 1 - \frac{n Z r_e}{\pi} \lambda^2 \quad (6)$$

$r_e = e^2/m_e c^2 \sim 2.8 \times 10^{-13}$ cm is the **classical electron radius**.

Imaging

$$n = \sqrt{1 - \frac{nZr_e}{\pi} \lambda^2} \sim 1 - \frac{nZr_e}{2\pi} \lambda^2 = 1 - \frac{\rho}{(Z/A)m_u} \frac{r_e}{2\pi} \lambda^2 =: 1 - \delta \quad (7)$$

Z : atomic number, A : atomic weight ($Z/A \sim 0.5$), ρ : density, $m_u = 1 \text{ amu} = 1.66 \times 10^{-24} \text{ g}$

Critical angle for X-ray reflection:

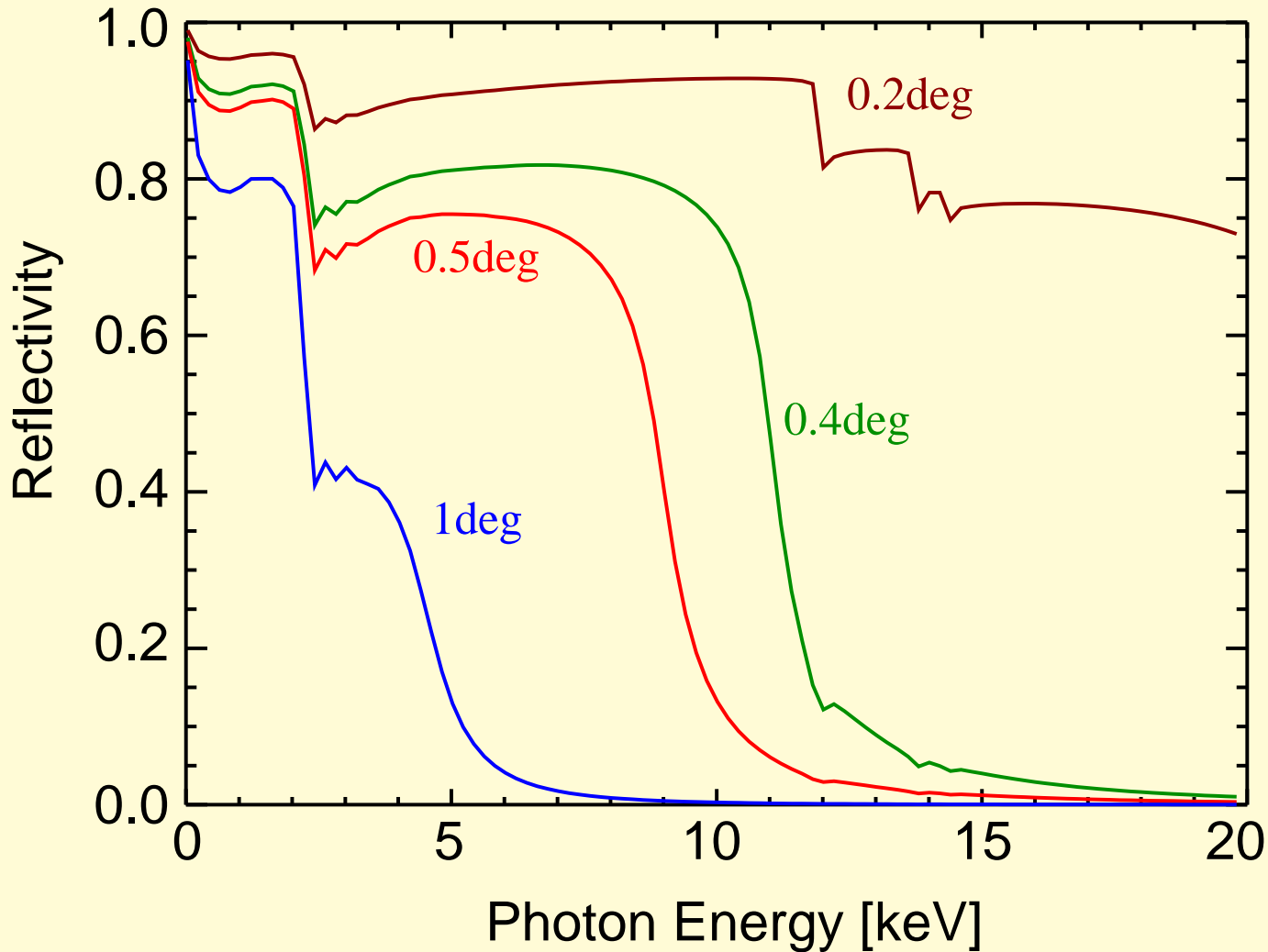
$$\cos \theta_c = 1 - \delta \quad (8)$$

Since $\delta \ll 1$, Taylor ($\cos x \sim 1 - x^2/2$):

$$\theta_c = \sqrt{2\delta} = 5.6' \left(\frac{\rho}{1 \text{ g cm}^{-3}} \right)^{1/2} \frac{\lambda}{1 \text{ nm}} \quad (9)$$

So for $\lambda \sim 1 \text{ nm}$: $\theta_c \sim 1^\circ$.

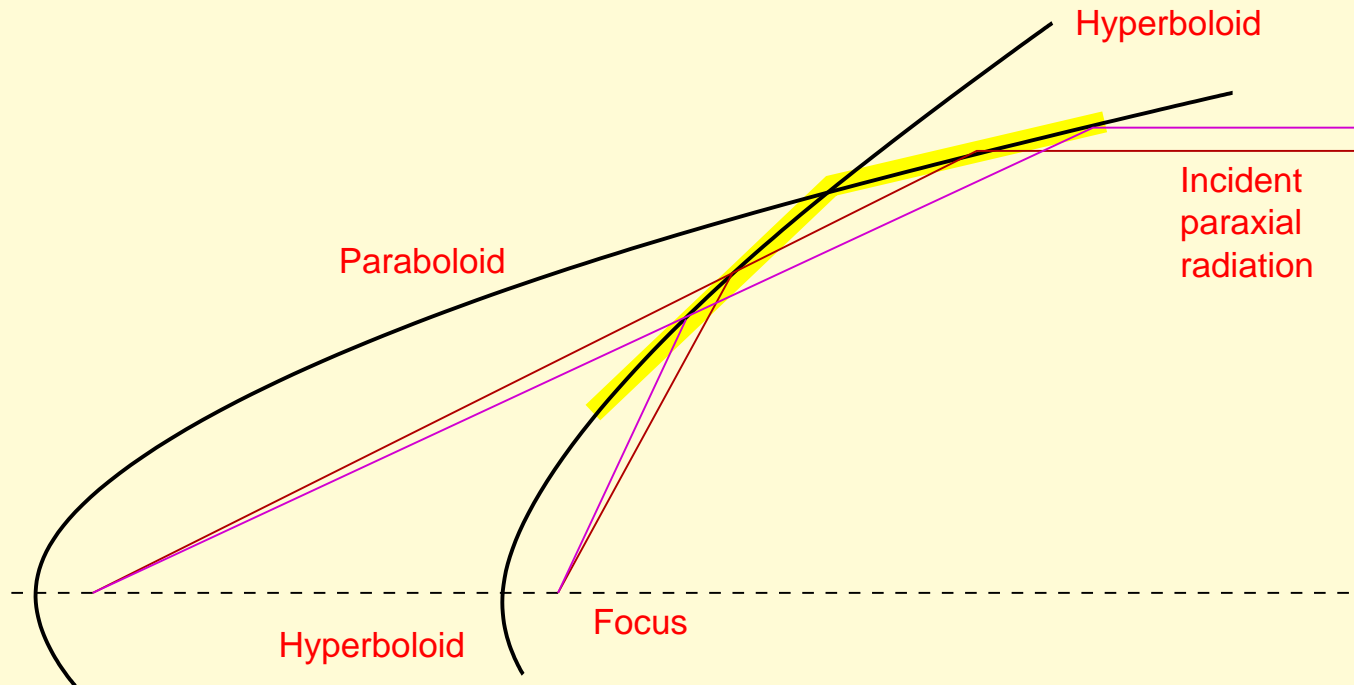
Imaging



Reflectivity for Gold

X-rays: Total reflection only works in the soft X-rays and only under grazing incidence
 ⇒ grazing incidence optics.

Imaging



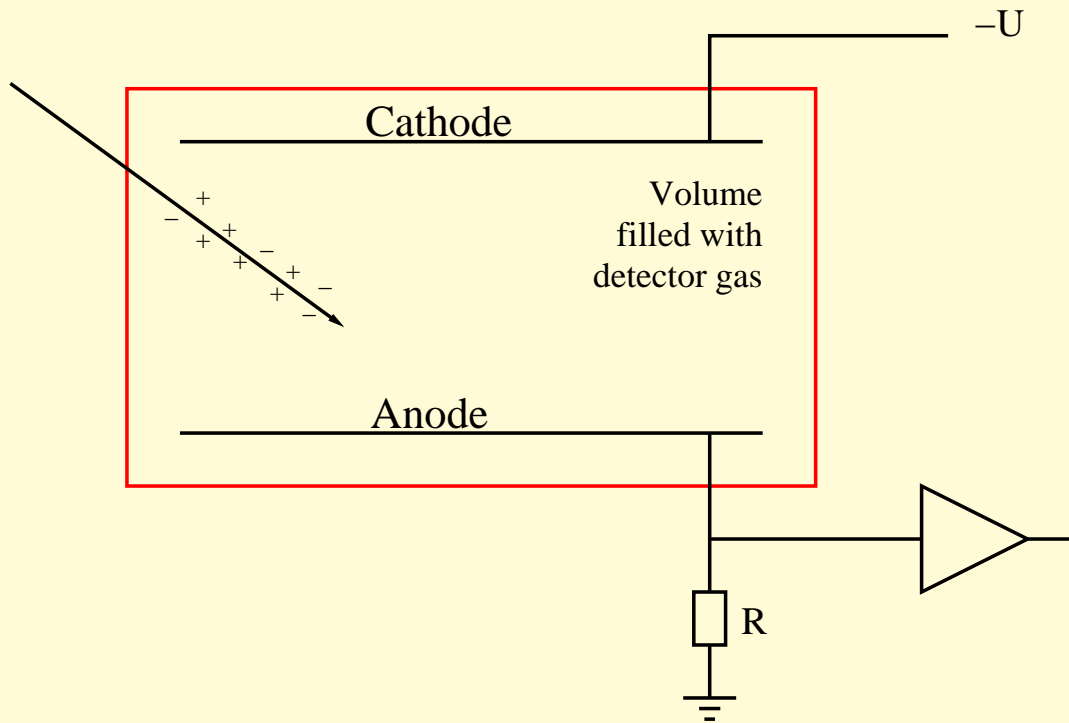
after ESA

To obtain manageable focal lengths (~ 10 m), do imaging with telescope using **two reflections** on a parabolic and a hyperboloidal mirror (“Wolter type I”)

(Wolter, 1952, for X-ray microscopes, Giacconi, 1961, for UV- and X-rays).

But: small collecting area ($A \sim \pi r^2 l / f$ where f : focal length), therefore one uses nested mirror shells (up to >50).

Ionization chamber



Simplest gas detector: gas-filled capacitor (**ionization chamber**)

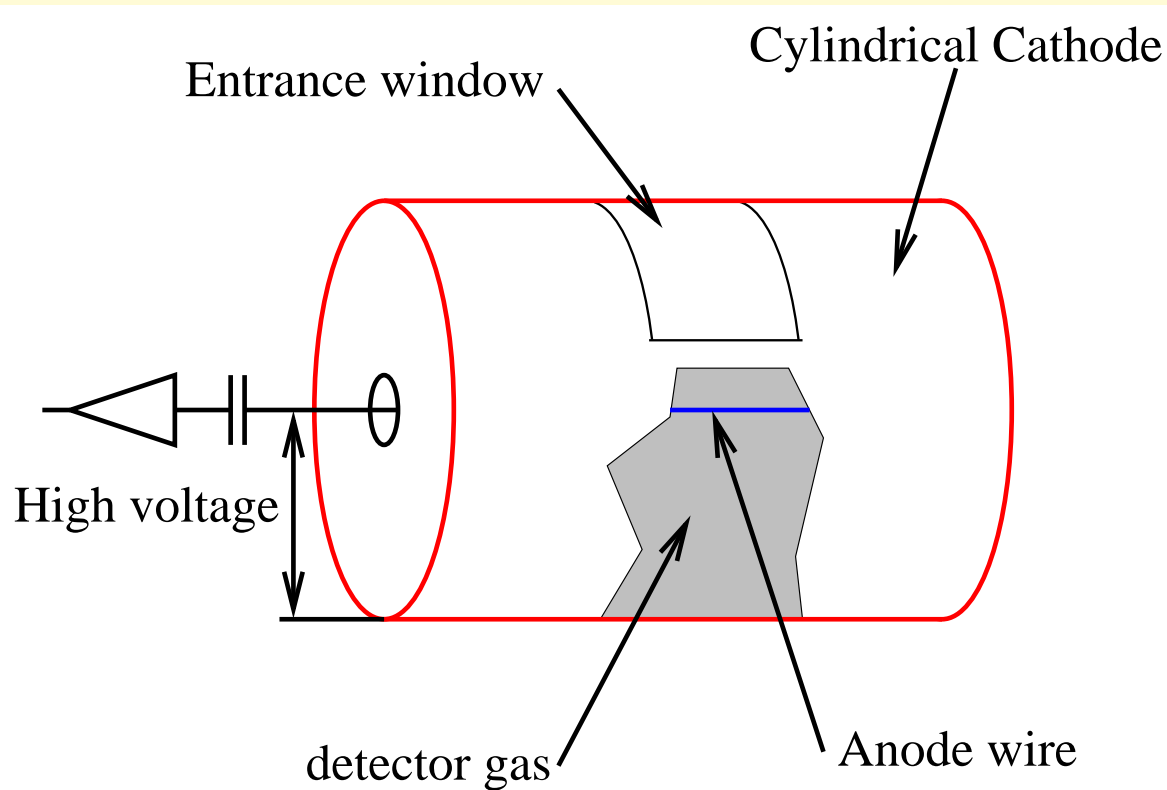
- photon is photo absorbed in detector gas
- K-shell electron ejected with energy \propto initial E
- through collisional ionization N charges are produced
- Electrostatic induction induces charge on capacitor plates
- Charge drains via R
 \implies Measurement

Pulse height: $\Delta Q = -Ne = C\Delta U \implies \Delta U = -Ne/C$

Typical magnitude of signal: $C = 20 \text{ pF}$, $Ne = 2 \times 10^5 e^- \cdot e \implies \Delta U = 1.6 \text{ mV}$.

\implies **Problem:** Pulse very weak since we are measuring the primary charge only.

Proportional Counters



Solution: **amplify charge**
 Close to Anode **wire**:

$$E(r) = V / (r \ln(b/a)) \quad (10)$$

(b radius of cathode, a radius of anode)

- ⇒ Strong **acceleration** of ionized particles
- ⇒ **Collisional ionization** of gas
- ⇒ **cascade!**

Measured voltage:

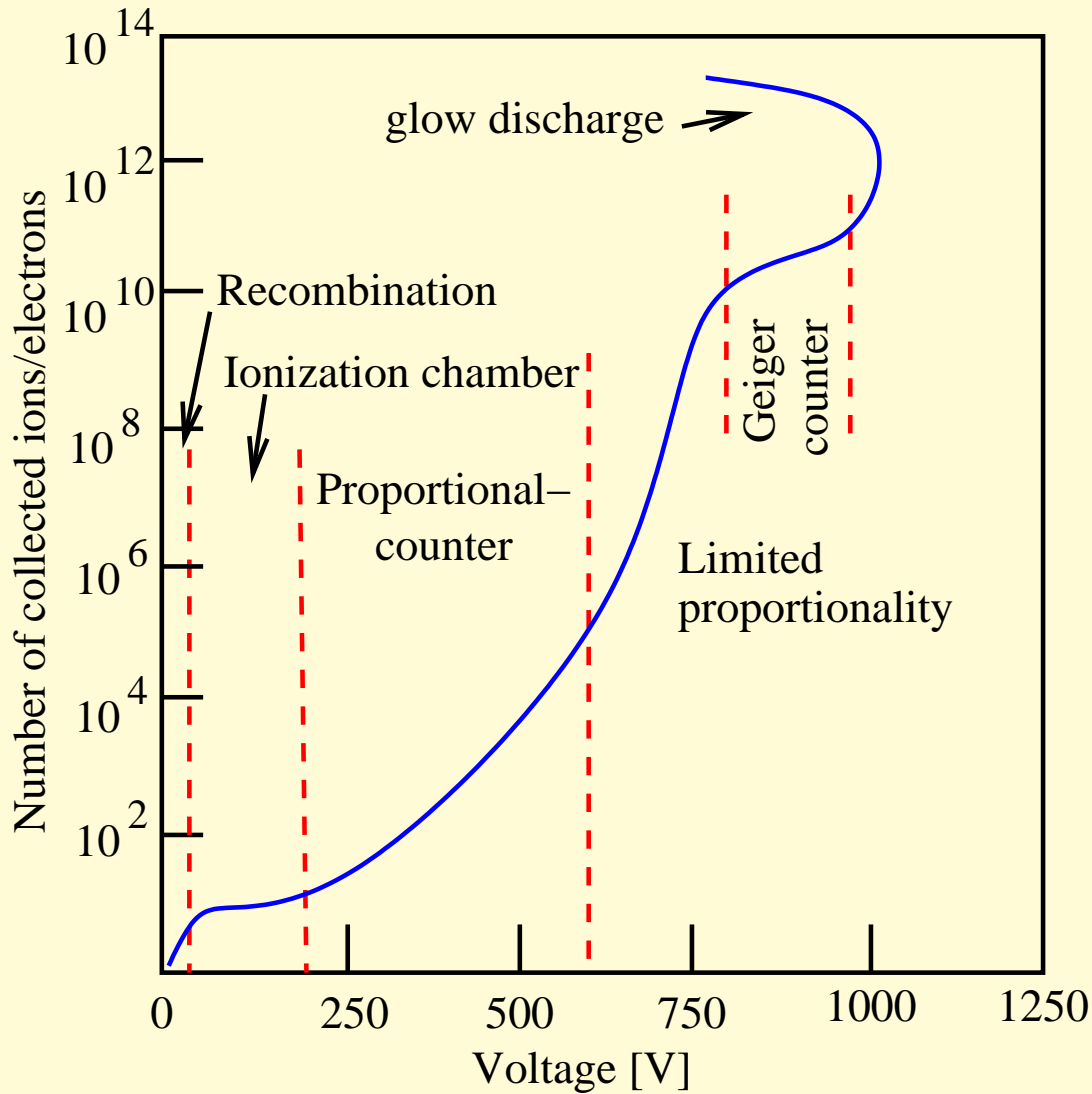
$$\Delta U = -\frac{eN}{C} \cdot A \quad (11)$$

where A : **amplification factor** (typically: $A = 10^4 \dots 10^6$).

Since $A \sim \text{const.}$: Voltage pulse $\propto N$, and therefore **Voltage pulse \propto detected X-ray energy!**

and therefore: “**proportional counter**”

Pulse Amplification



Pulse amplification in detector as a function of anode voltage.

Typical proportional counter voltages are several 100 to 1000 V (depending on detector gas).

(after Grupen, Fig.4.21)

Detector Gas

Use **inert gases**, e.g., Ar or Xe, since required voltage smallest and only low losses due to excitation of the gas atoms.

Number of ions produced: $N = E/\omega$, where ω is given by:

Gas	H	He	Ne	Ar	Kr
ω [eV]	36.6	44.4	36.8	26.25	24.1
Gas	Xe	Air	CO ₂	CH ₄	
ω [eV]	21.9	35.2	34.2	29.1	

⇒ Typically $N \sim 1000$ **electron-ion pairs** per 20 keV photon.

Note:

- probability for absorption $\sigma_{\text{bf}} \propto Z^{4...5}$
⇒ use **Xenon** ($Z = 54$) for astronomical detectors
- since $\sigma_{\text{bf}} \propto E^{-3}$
⇒ **proportional counters limited to $E < 100$ keV.**

Energy Resolution

Measured signal: pulse height \implies Energy of the X-ray

Resolution: ΔE : Width (=FWHM, Full Width at Half Maximum) of the distribution of measured energies.

Poisson statistics (N discrete Electron-Ion pairs!):

$$\Delta E \propto 2.35\sqrt{N} \propto 2.35\sqrt{E} \quad (12)$$

Slight correlations due to amplifying discharge \implies Variance somewhat smaller than expected from Poisson statistics \implies described with **Fano Factor** F :

$$\frac{\Delta E}{E} = 2.35 \left(\frac{F}{N} \right)^{1/2} \quad (13)$$

where for gas detectors $F \sim 0.2-0.3$

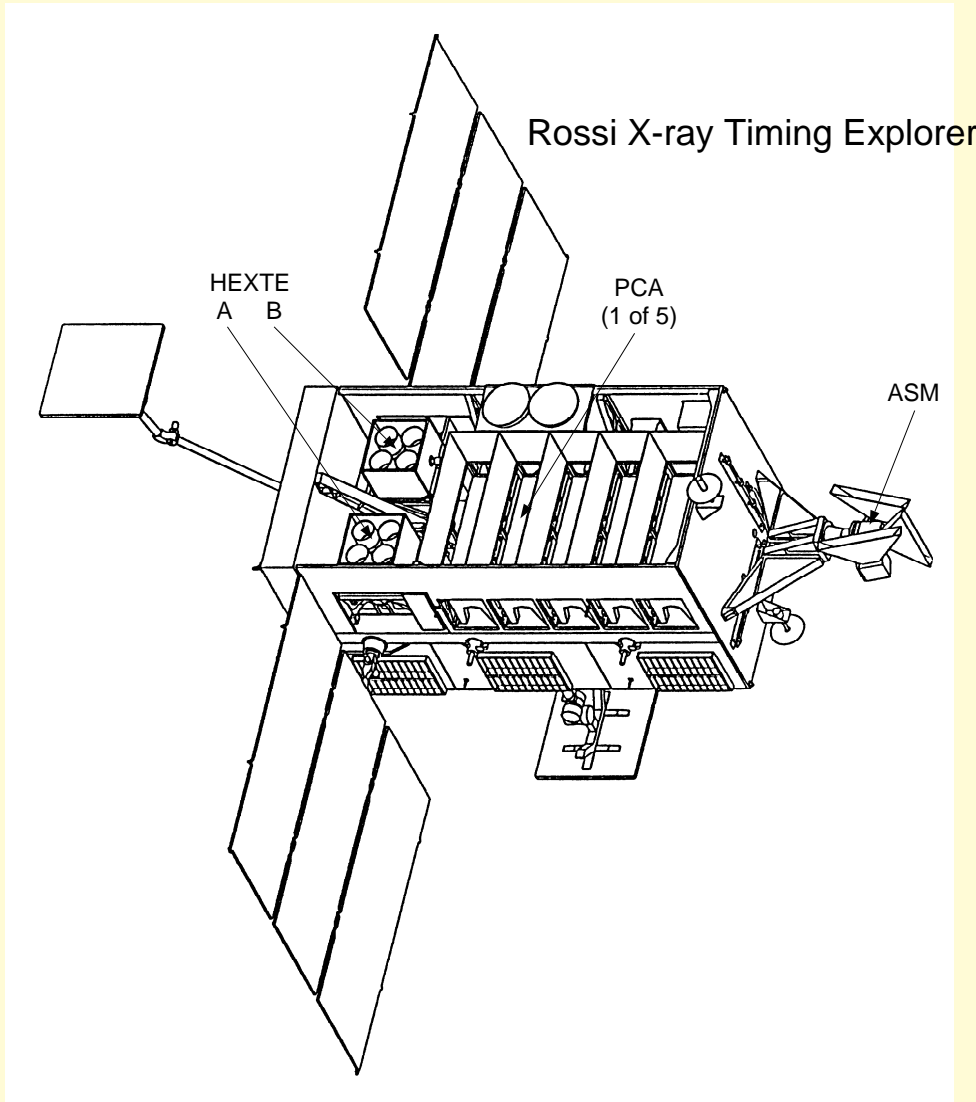
More detailed theory yields

$$\frac{\Delta E}{E} = 2.35 \left(\frac{W(F+A)}{E} \right)^{1/2} \quad (14)$$

W : mean energy to produce a pair (26 eV for Ar+Methane), $F \sim 0.2$, $A \sim 0.6$

\implies up to 14% at 5.9 keV doable.

Example: RXTE-PCA

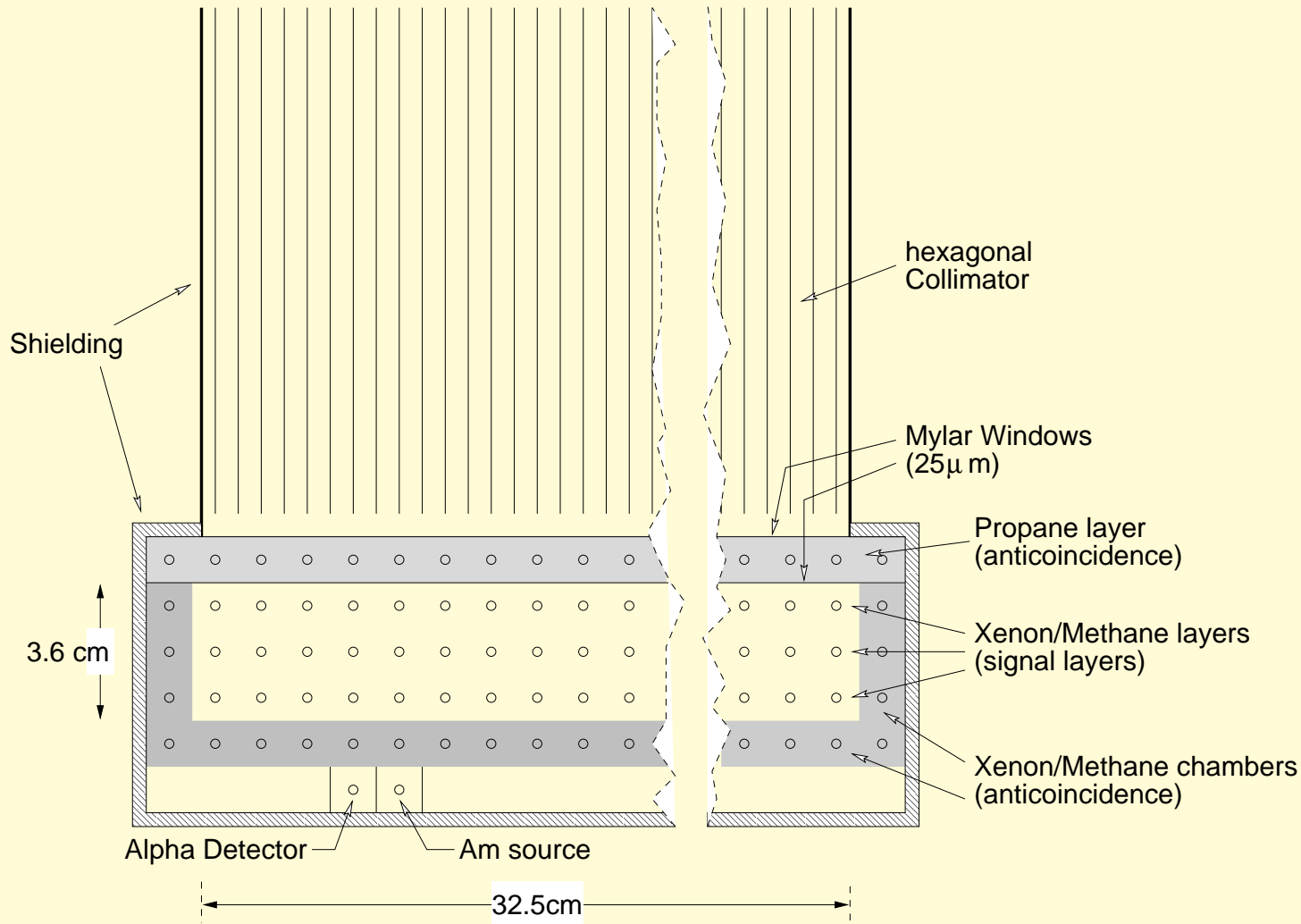


Rossi-X-ray Timing Explorer, Launch 30.12.1995, 3 instruments:

- Proportional Counter Array (PCA, 2–100 keV),
- High Energy X-ray Timing Experiment (HEXTE, 15–250 keV),
- All Sky Monitor (ASM, 2–10 keV)

PCA and HEXTE have μsec timing resolution

Example: RXTE-PCA



PCA consists of 5 Proportional Counter Units (PCUs), 1 atm pressure

Propane and outer anodes in **Anti-Coincidence** ⇒ Background reduction

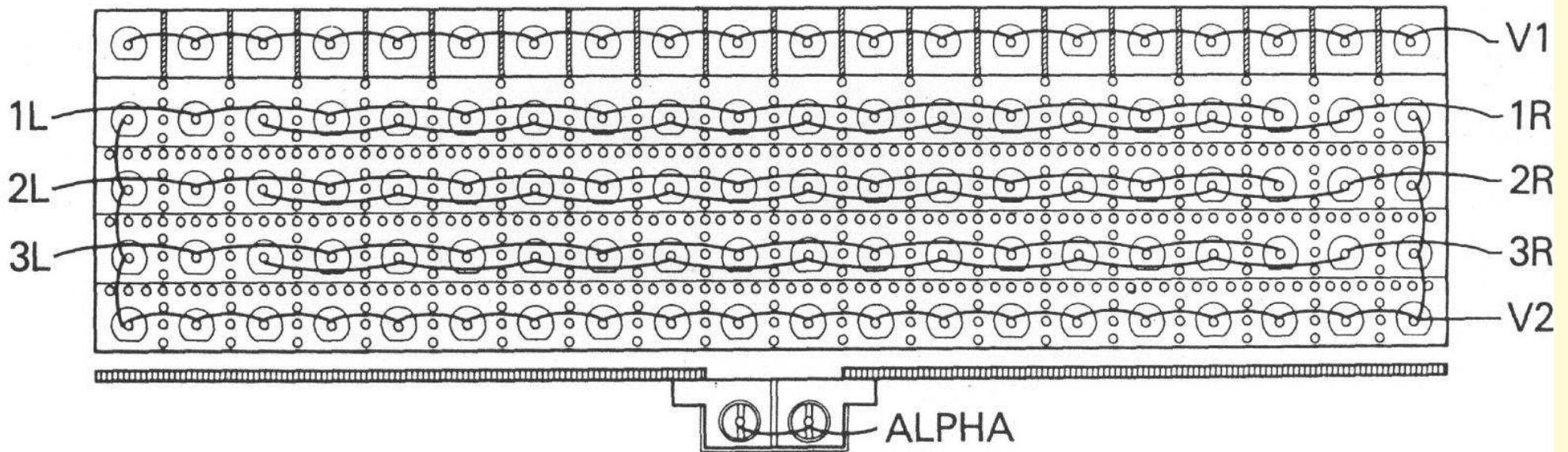
BeCu-Collimator to limit field of view to $\sim 1^\circ$

^{241}Am -source for energy calibration

(simultaneous emission of 59.6 keV γ 's and α -particles ⇒ coincidence measurements).

Example: RXTE-PCA

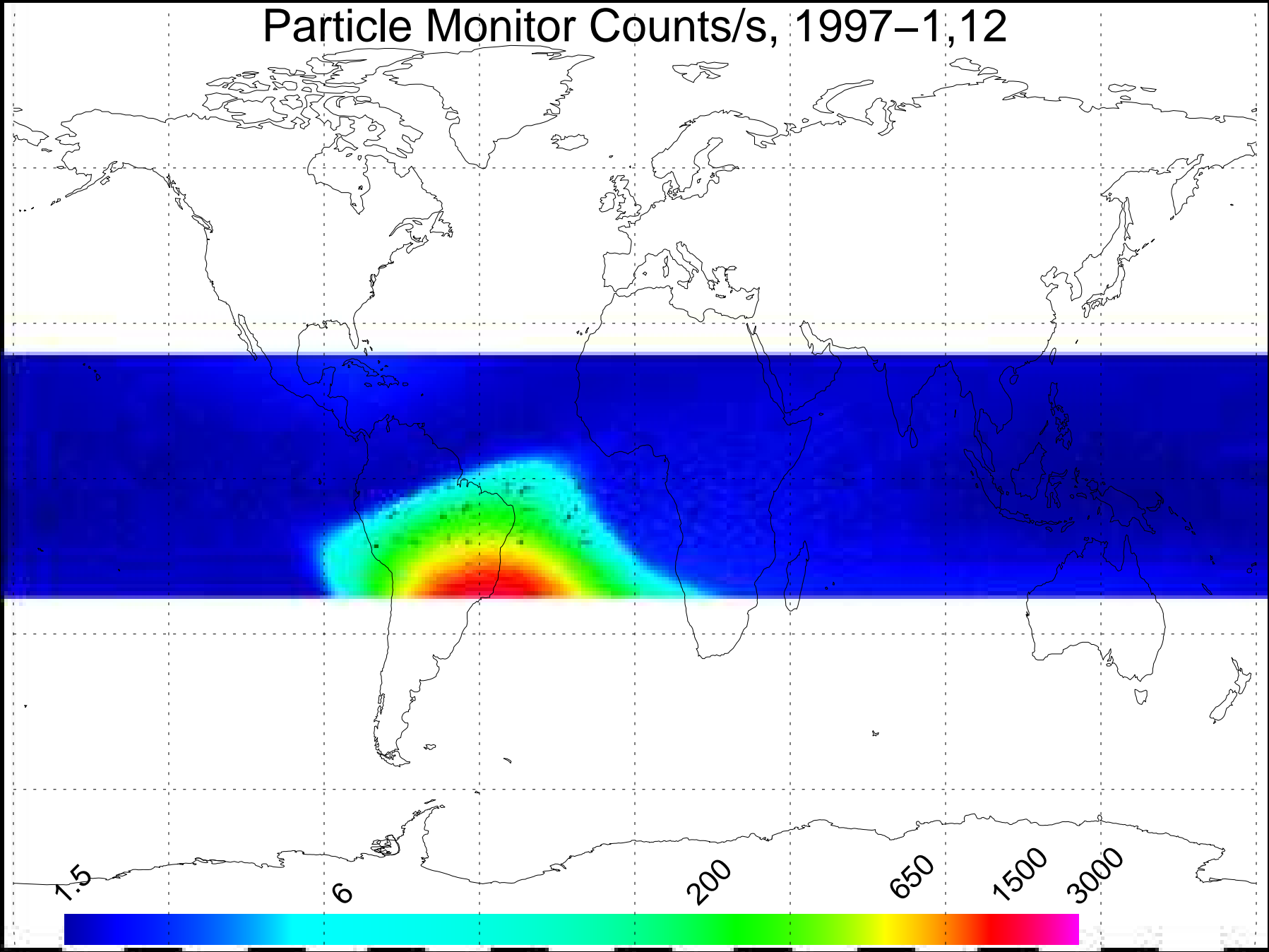
COLLIMATOR



(Jahoda et al., 2006)

Wiring schematics of one proportional counter unit of the *RXTE*-PCA;
V2 is the veto anode

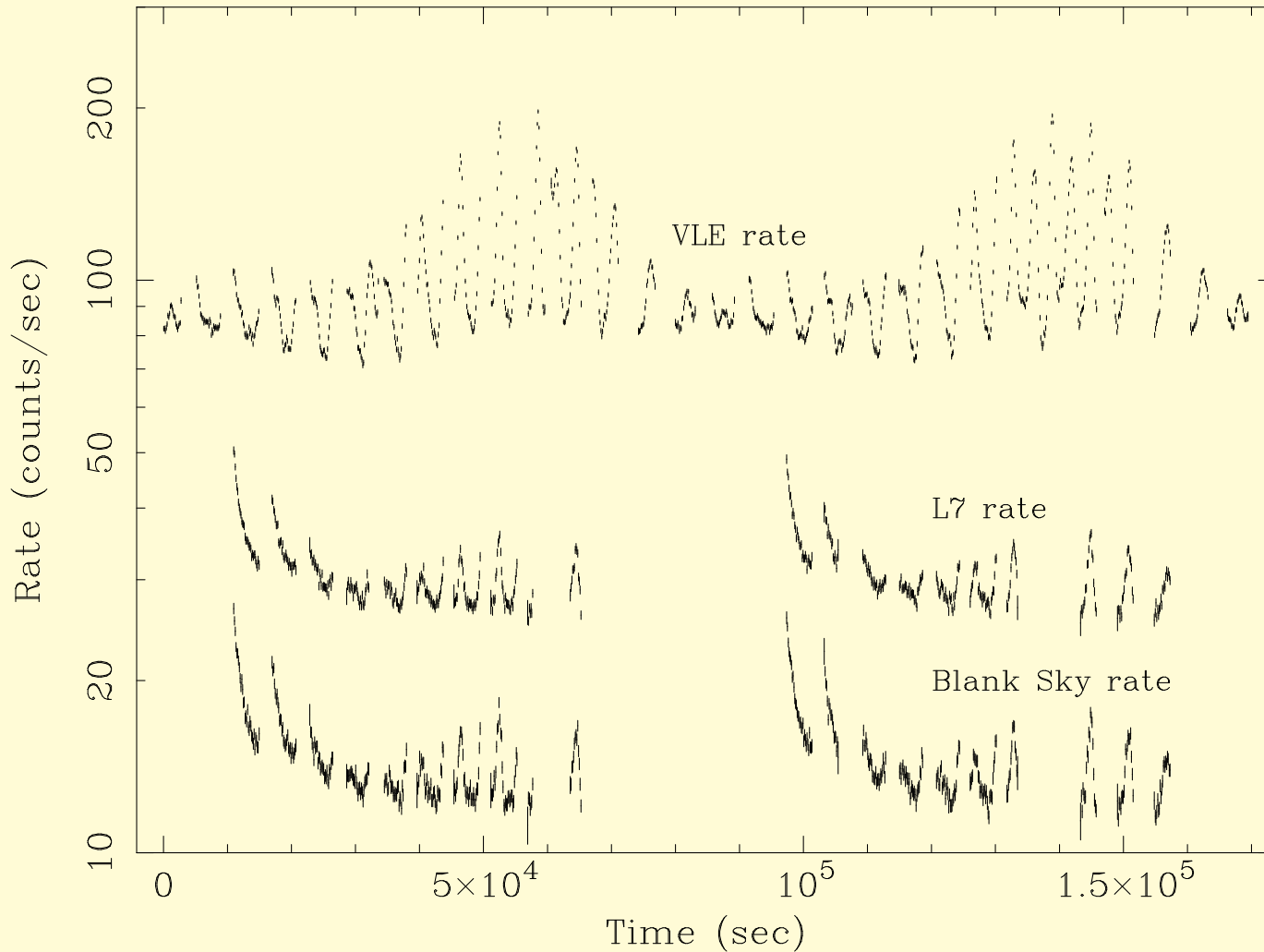
Particle Monitor Counts/s, 1997–1,12



(Fürst et al., 2009)

Background at ~ 500 km height: note the South Atlantic Anomaly

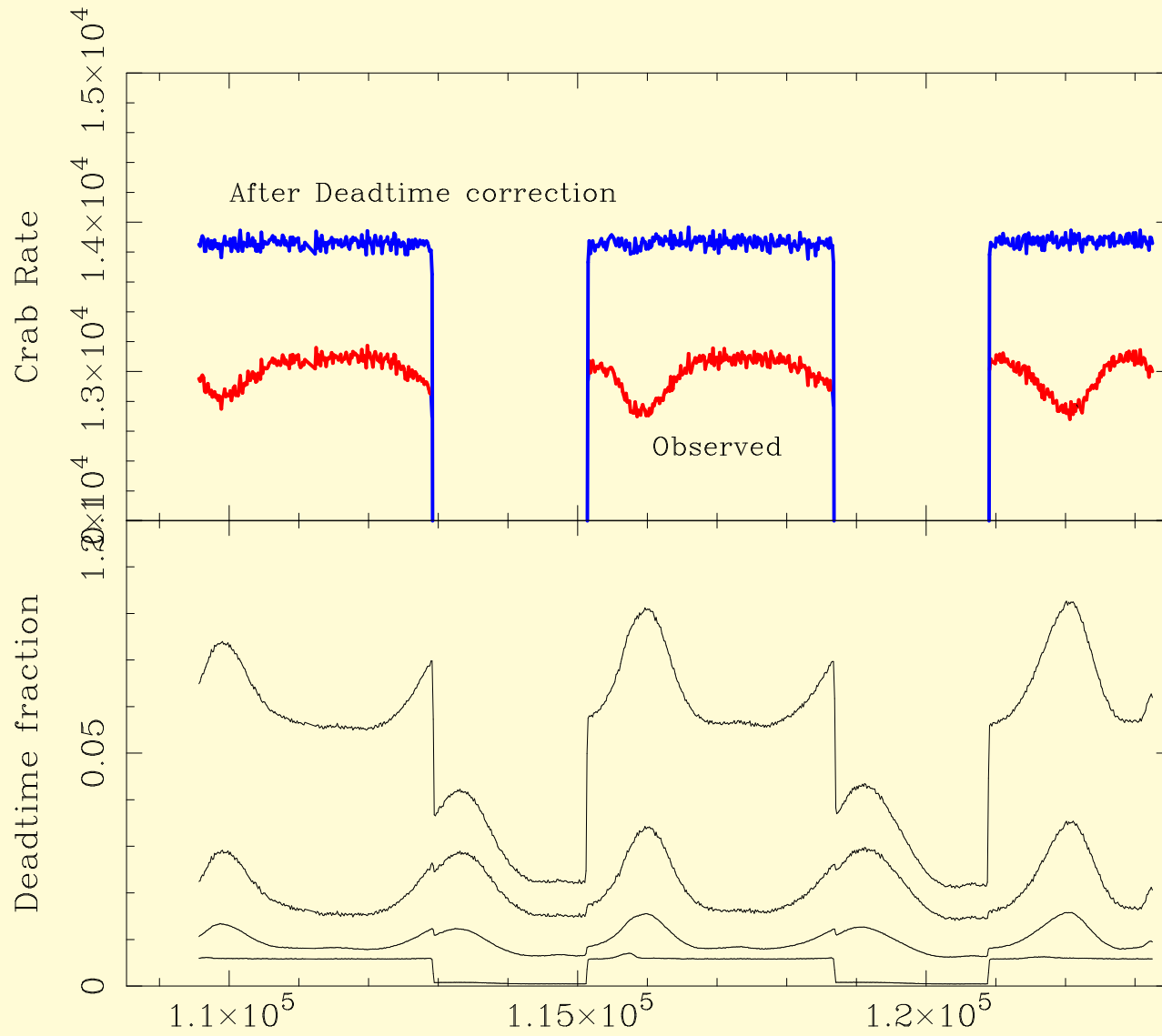
Example: RXTE-PCA



High-energetic particles produce a **strong and time-varying background** in the detector.

Jahoda et al. (2006;
Fig. 25)

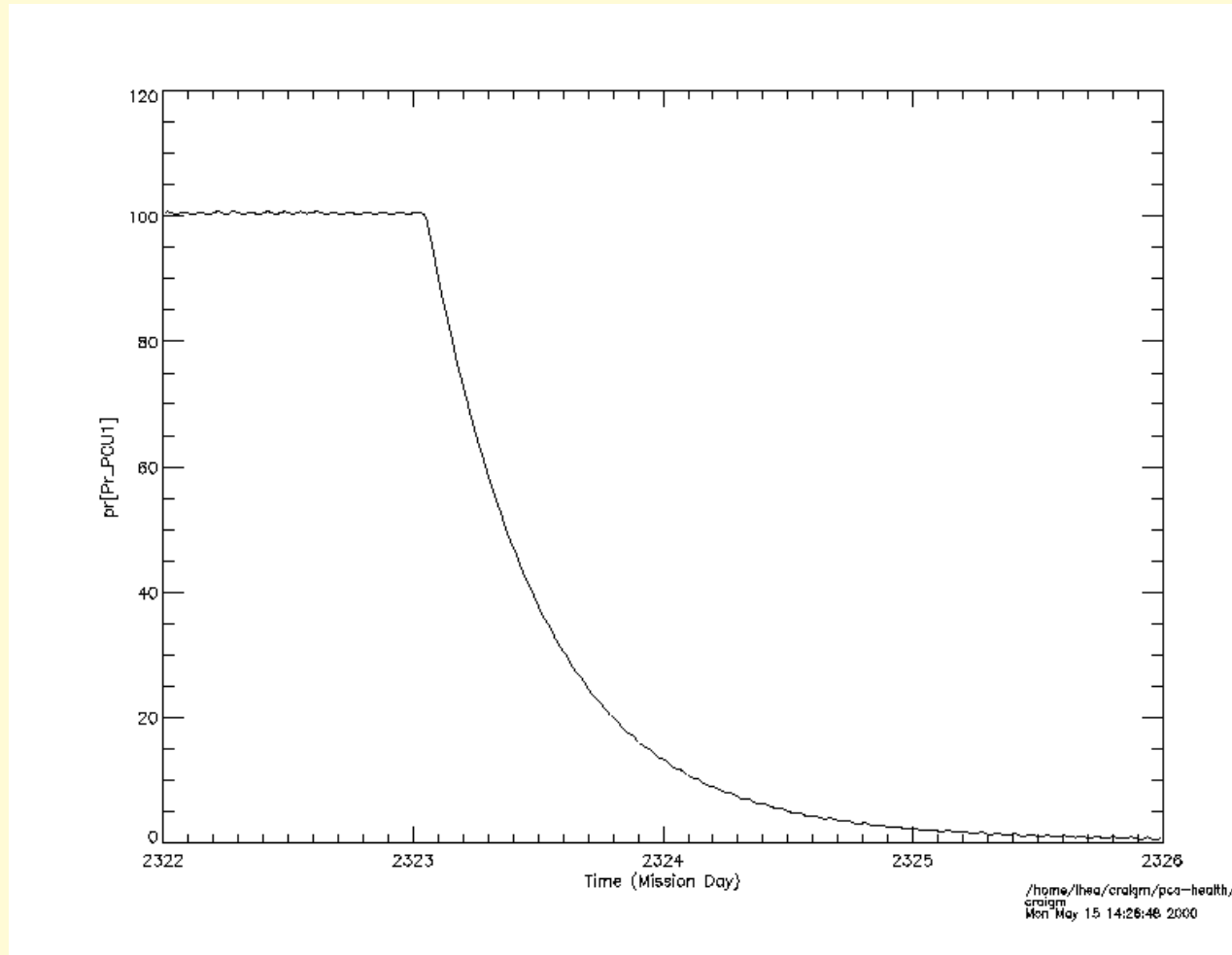
Example: RXTE-PCA



Non-photon events due to particle background of the satellite cause **deadtime** in the detector countrate which has to be corrected.

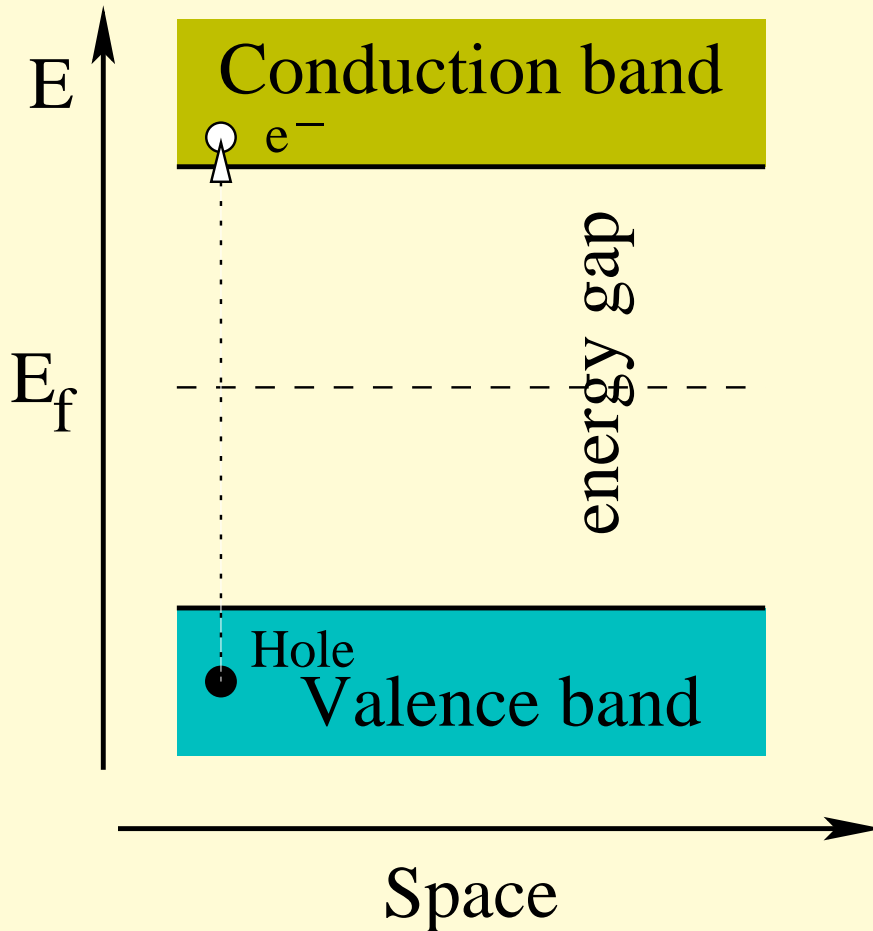
Jahoda et al. (2006; Fig. 30)

Example: RXTE-PCA



... this is what happens once a Mylar window starts having a hole in space

X-ray CCDs



Semiconductors: separation of **valence band** and **conduction band**
 ~ 1 eV (=energy of visible light).

Absorption of photon in Si: Energy of photon released

Number of electron-hole pairs produced:

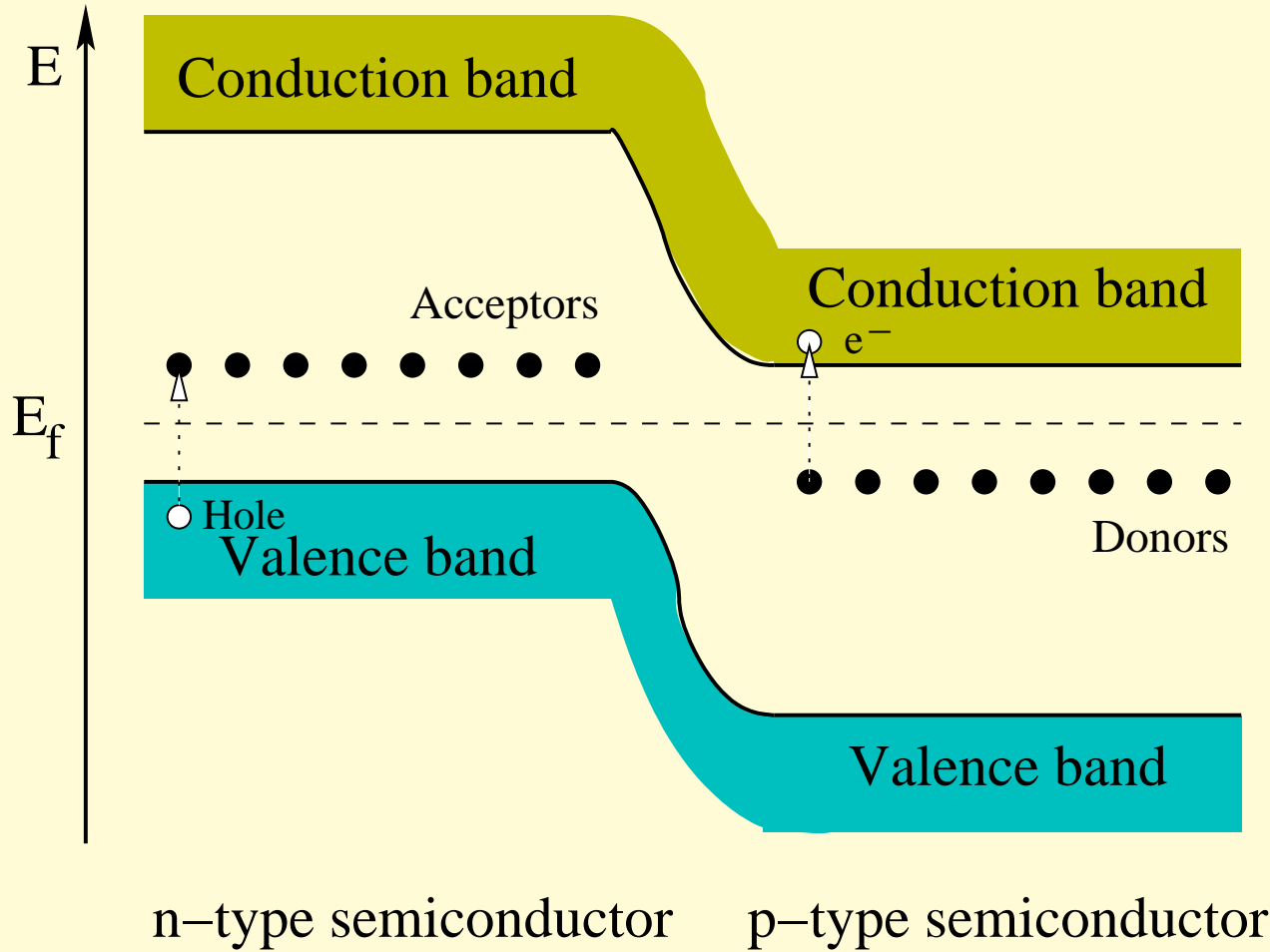
$$N \sim \frac{h\nu}{E_{\text{gap}}} \quad (15)$$

in other words:

- optical light: ~ 1 electron-hole pair
- X-rays (keV): ~ 1000 electron-hole pairs

Problem: electron-hole pairs recombine immediately in a normal semiconductor.

X-ray CCDs



“Doping” the semiconductor moves the valence- and conduction bands.

Connecting a “n-type” and a “p-type” semiconductor gives a **pn-junction**.

Electron-hole pairs created at pn-junction will be separated by field gradient

⇒ electrons can then be collected in potential well away from the junction and read out.

X-ray CCDs

Interaction of X-ray with Si: number of electrons produced

$$n_{\text{electrons}} = \frac{E}{\Delta E_{\text{gap}}} \sim \mathcal{O}(1000) \quad (16)$$

⇒ if electrons are detected individually by fast read out of CCD, then the CCD is a X-ray spectrometer *and* imager

bright sources: several 1000 photons per second ⇒ readout in μs !

Typical energy resolution reached today:

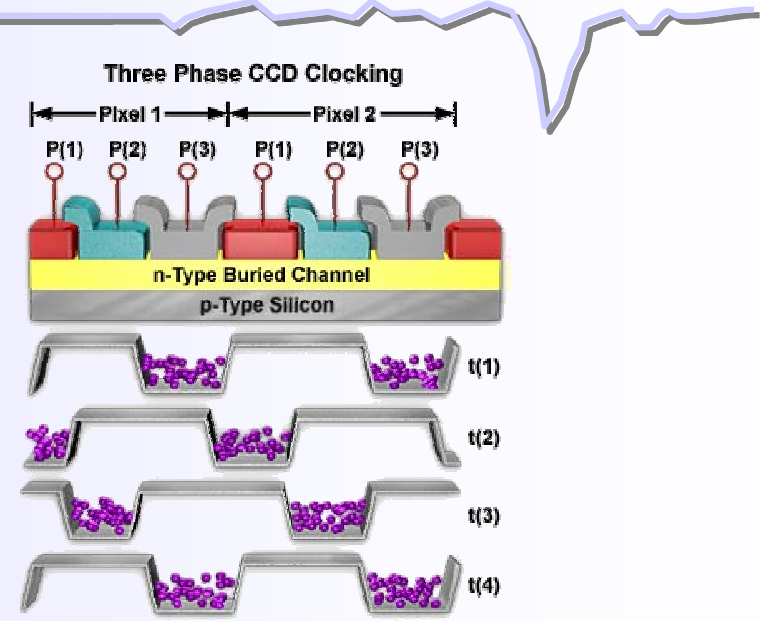
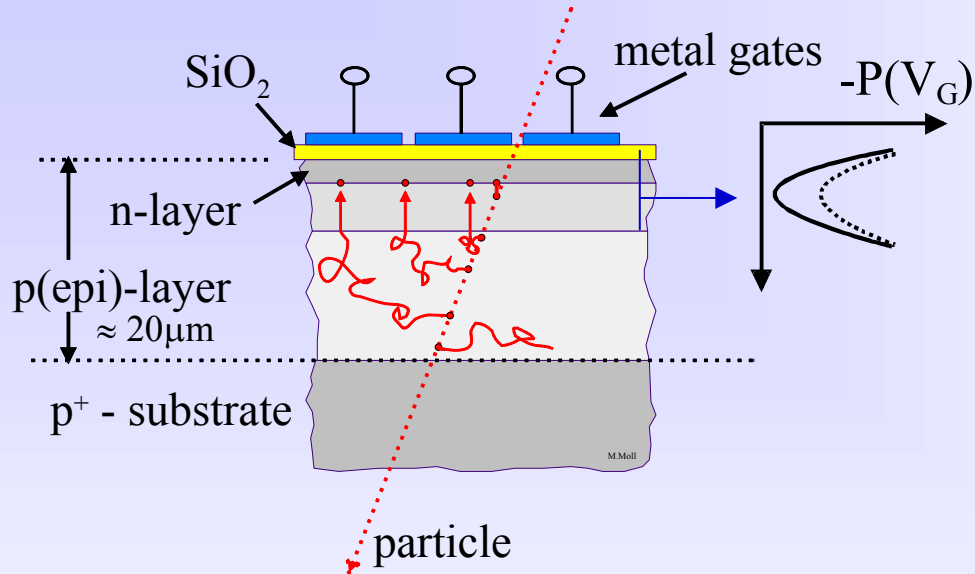
$$\frac{\Delta E}{E} = 2.355 \sqrt{\frac{3.65 \text{ eV} \cdot F}{E}} \quad (17)$$

with $F \sim 0.1 \Rightarrow \Delta E/E \sim 0.4\%$, so **much better than proportional counters**.

(but same $\Delta E/E \propto E^{-1/2}$ proportionality because of Poisson!)

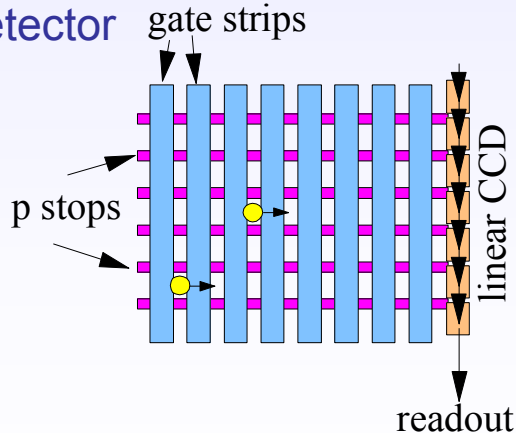
Since the sensitivity is close to 100%: Si based CCDs are currently the best available imaging photon detectors for optical and X-ray applications.

(1) MOS structure with segmented metal layer;
Charge is captured in a potential well.



(2) Readout: Shift electrons towards anode by periodic variation of 3 potentials

(3) Create an array of pixel for a 2D detector

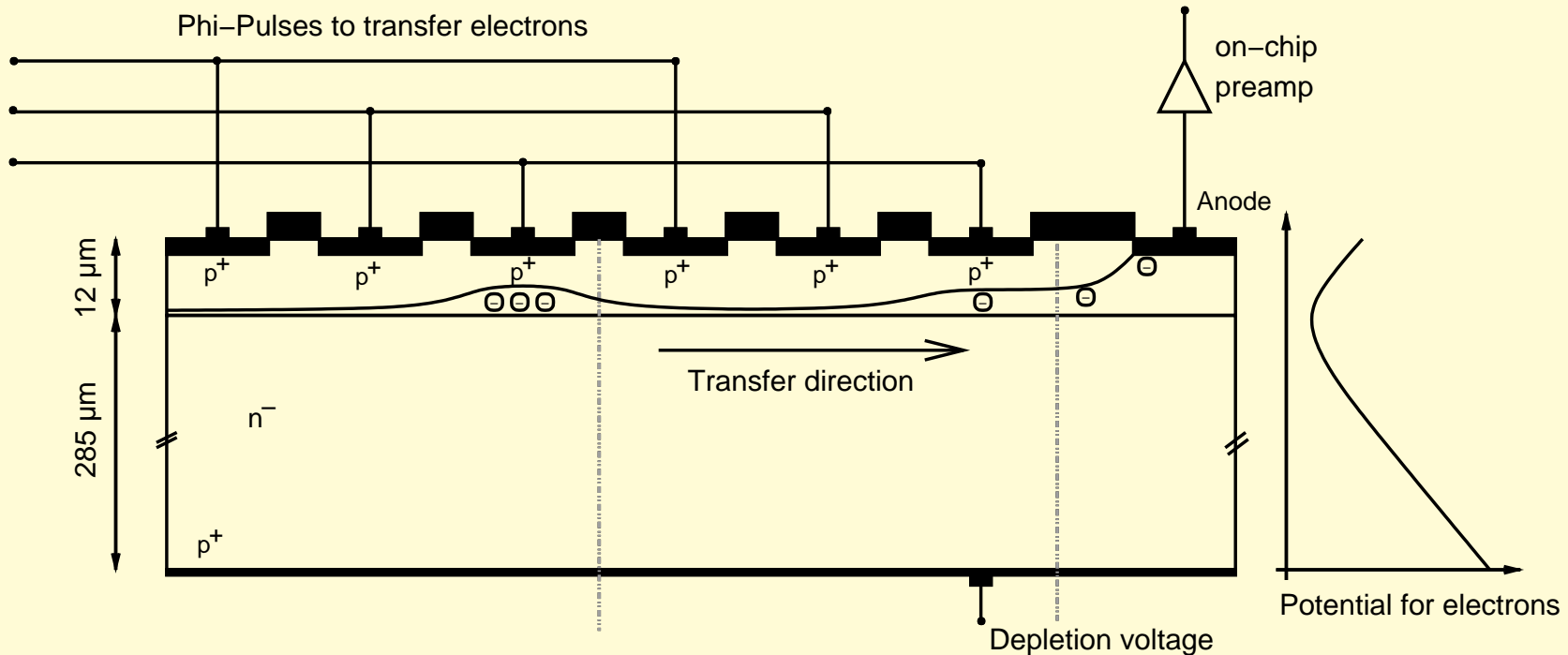


Pixel CCD

- needs only few readout channels
- small charge ($\approx 2000 e$) \Rightarrow needs cooling
- long readout time, active during readout
- sensitive to radiation damage

\Rightarrow applicable for low rate experiment without high intensity radiation field

X-ray CCDs

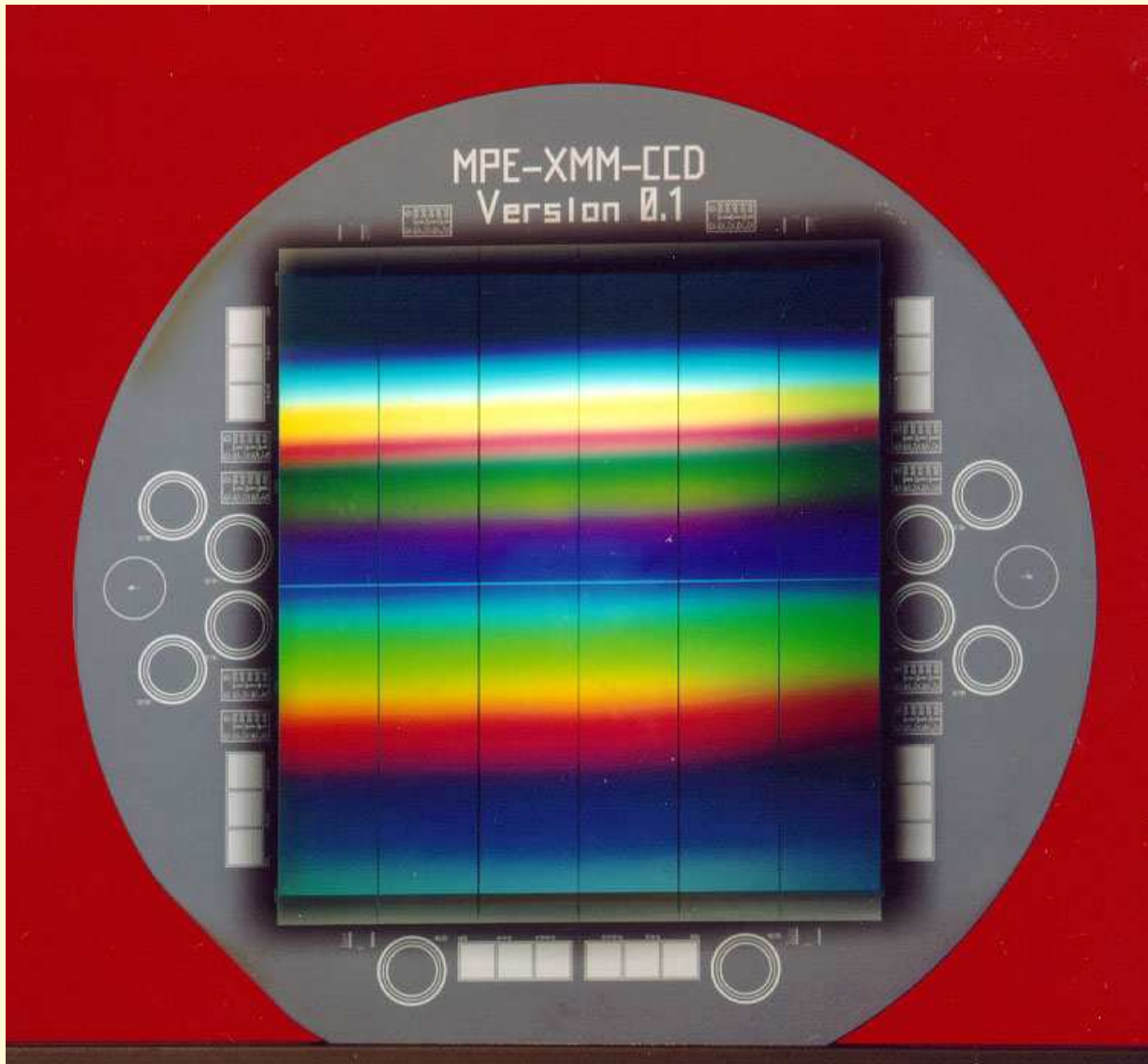


Schematic structure of the *XMM-Newton* EPIC pn CCD.

Problem: Infalling structure has to pass *through* structure on CCD surface \implies loss of low energy response, also danger through destruction of CCD structure by cosmic rays. . .

Solution: Irradiate the back side of the chip. Deplete whole CCD-volume, transport electrons to pixels via adequate electric field (“**backside illuminated CCDs**”)

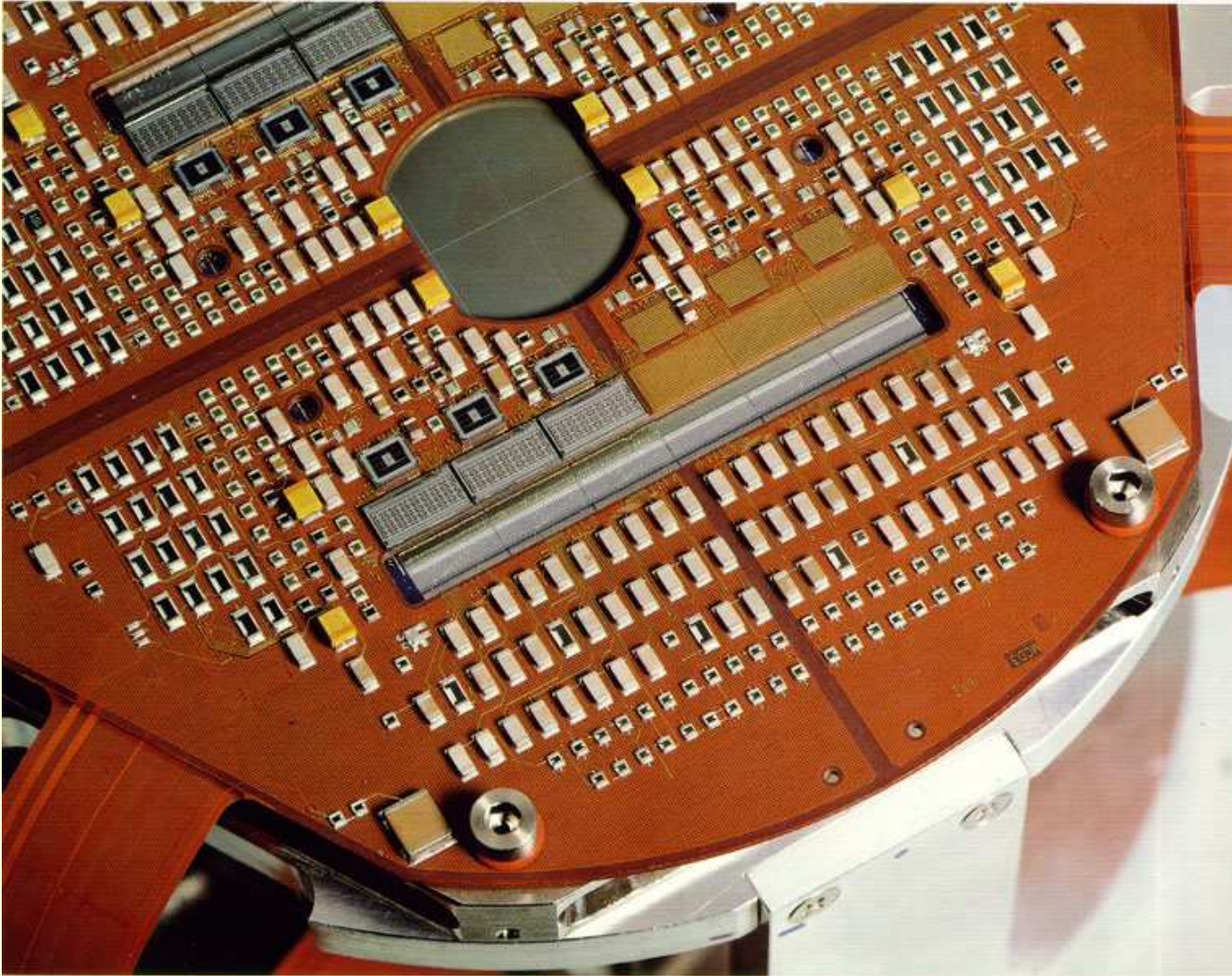
XMM-Newton: EPIC-pn CCD



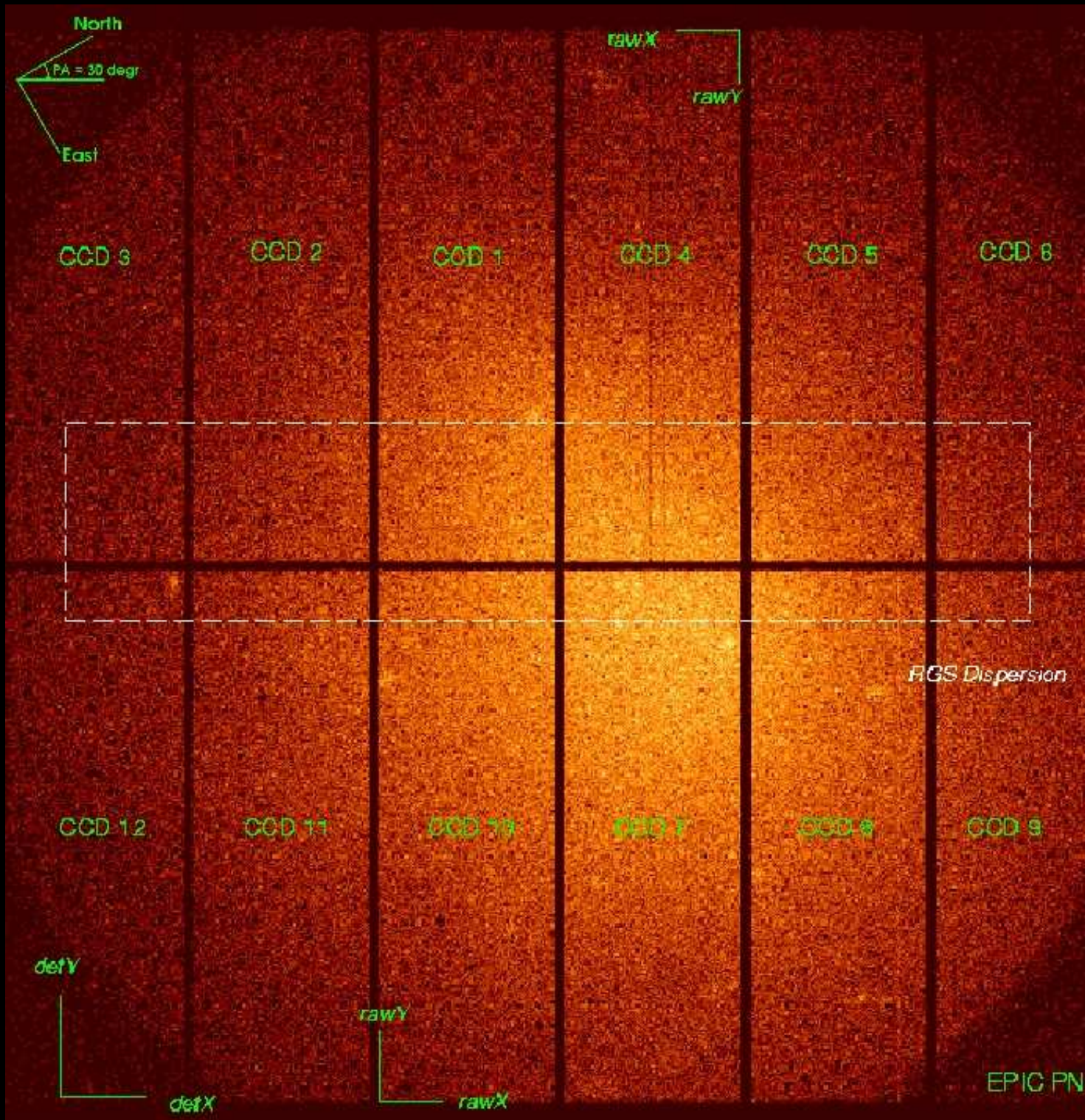
XMM-Newton: Array of individual backside illuminated CCDs on one Silicon wafer \implies requires extreme care during production

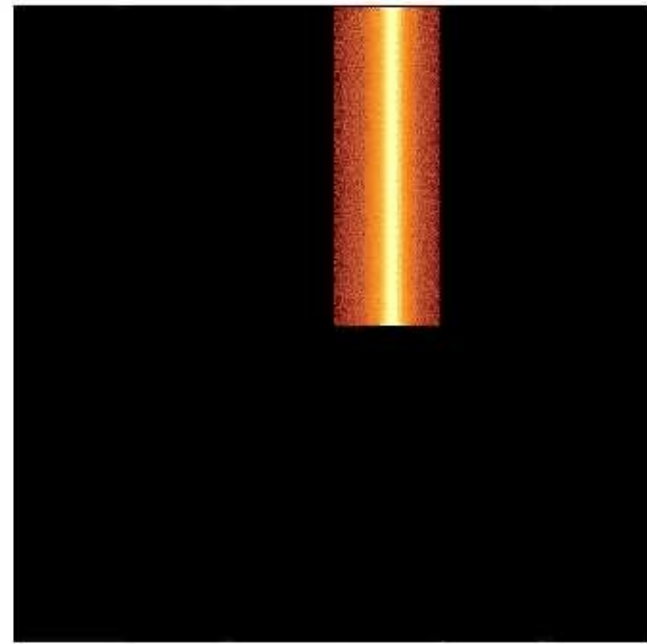
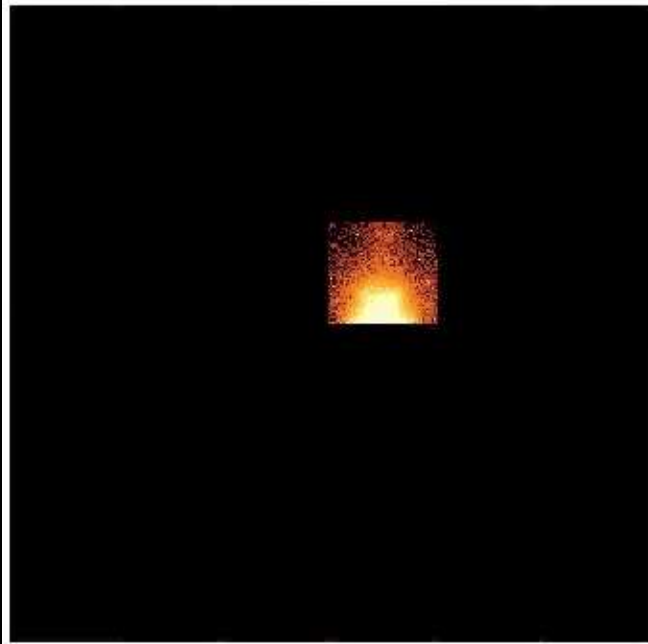
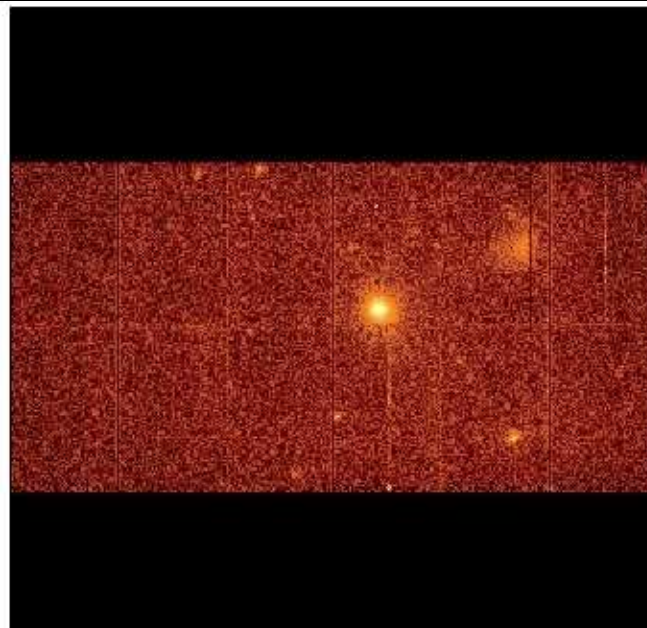
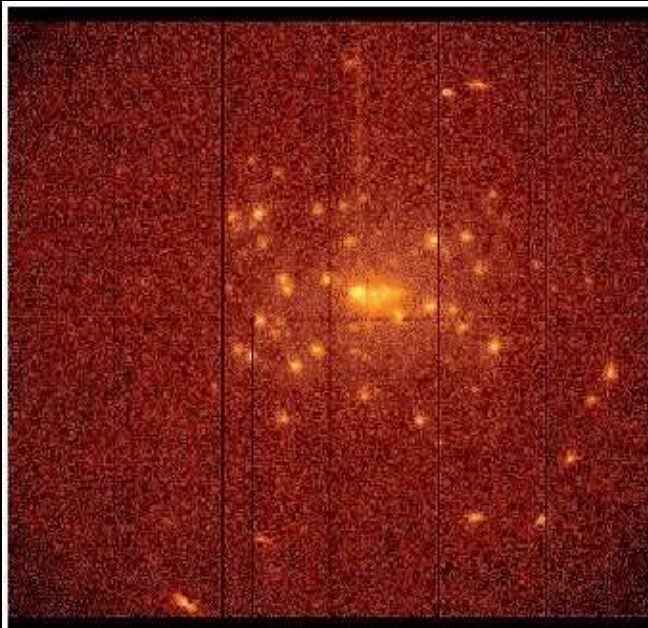
at the time of production one of the most complex Silicon structures ever made (diameter: 65.5 mm)

XMM-Newton: EPIC-pn CCD



Backside of the
EPIC-pn camera
head



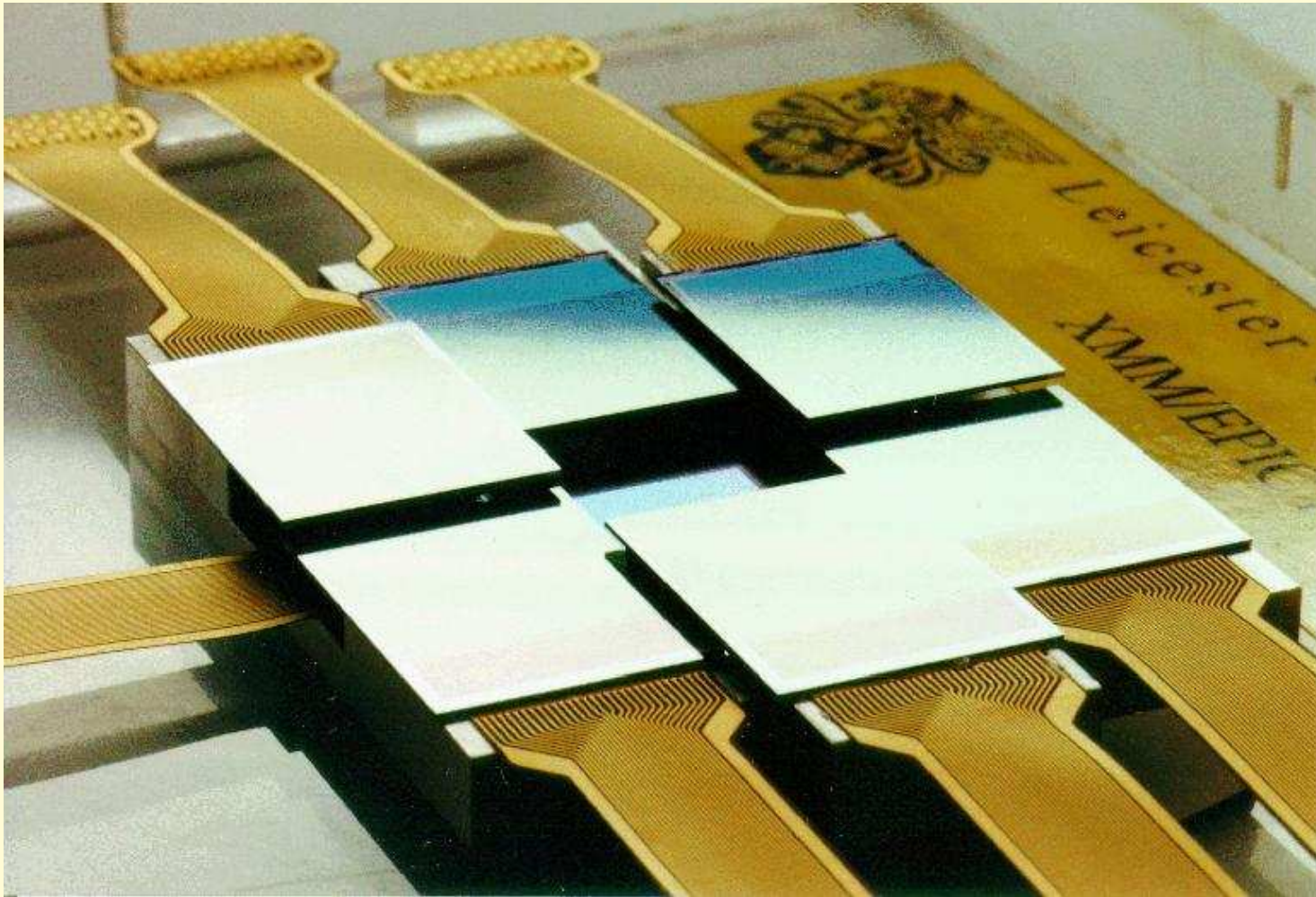


Different read out strategies can be used to speed up the read out in case bright sources are observed to allow X-ray timing and to avoid pile-up:

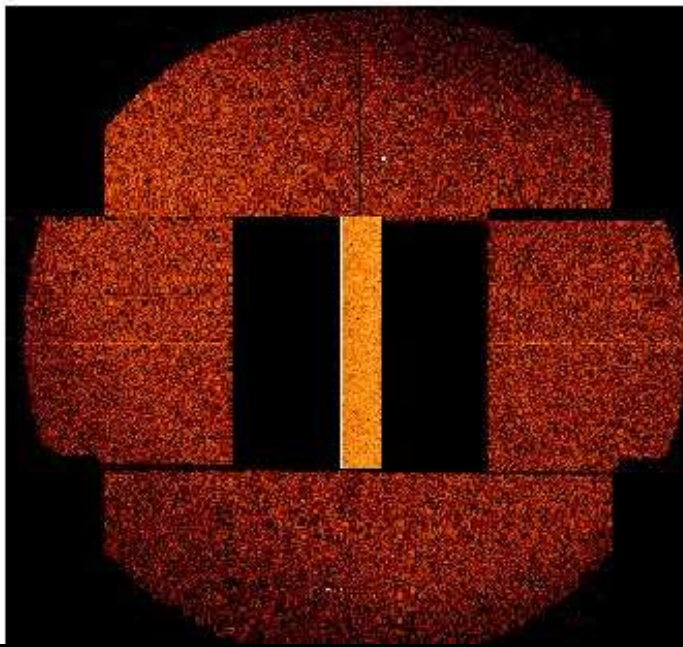
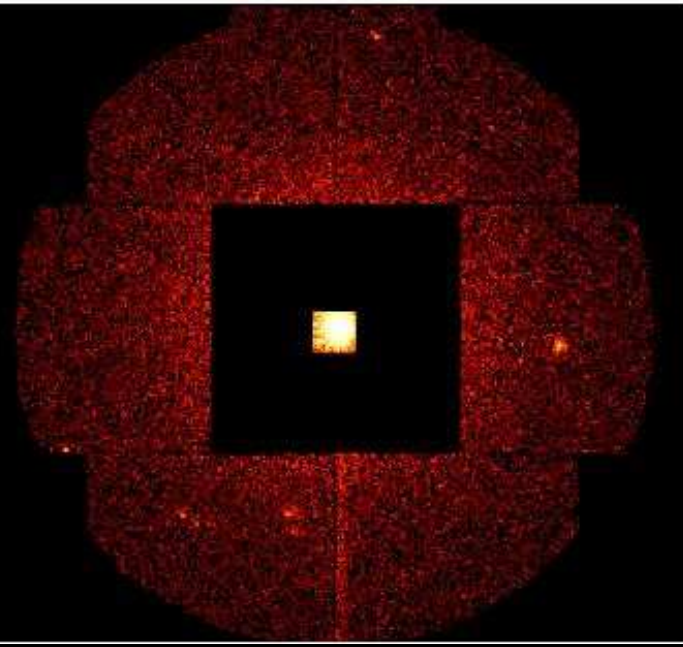
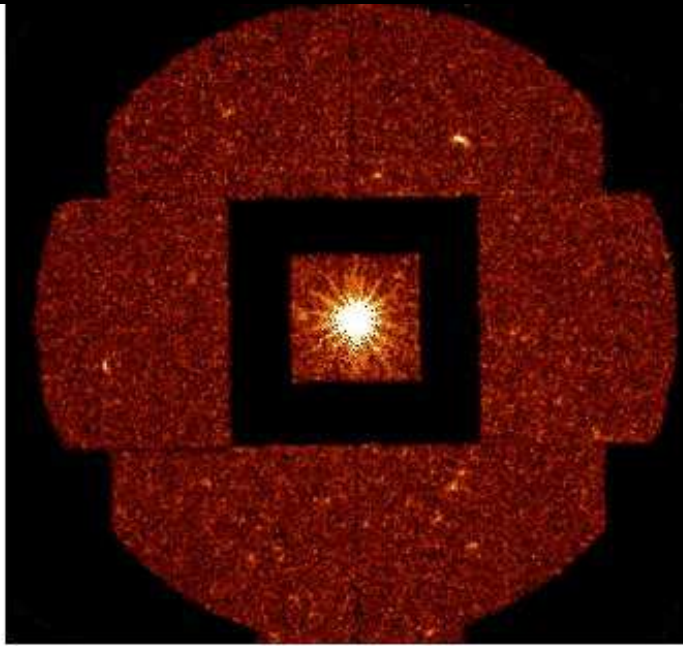
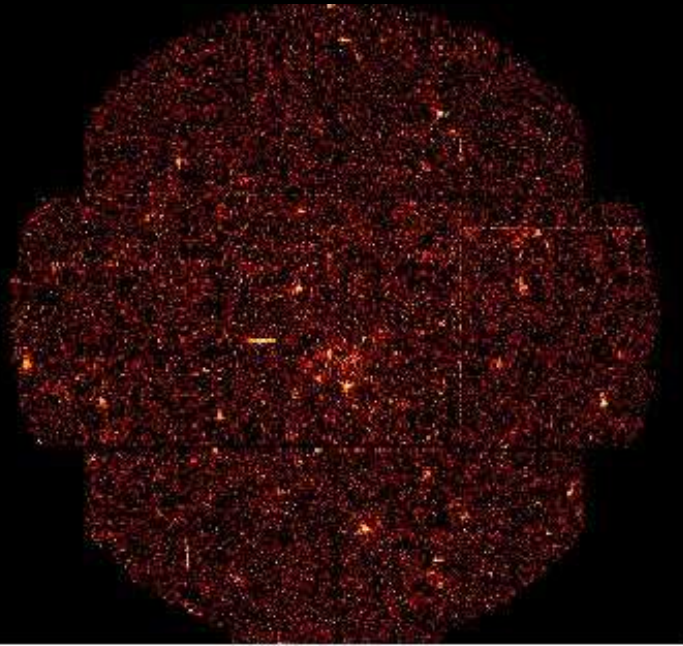
- Full frame mode:
 376×384 ,
 $\Delta t = 73 \text{ ms}$
- Large Window mode:
 198×384 ,
 $\Delta t = 48 \text{ ms}$
- Small Window mode:
 63×64 , $\Delta t = 6 \text{ ms}$
- Timing Mode:
 64×200 ,
 $\Delta t = 0.03 \text{ ms}$
- Burst Mode: 64×180 ,
 $\Delta t = 7 \mu\text{s}$, but only
3% efficiency

ESA

XMM-Newton: EPIC-MOS CCD

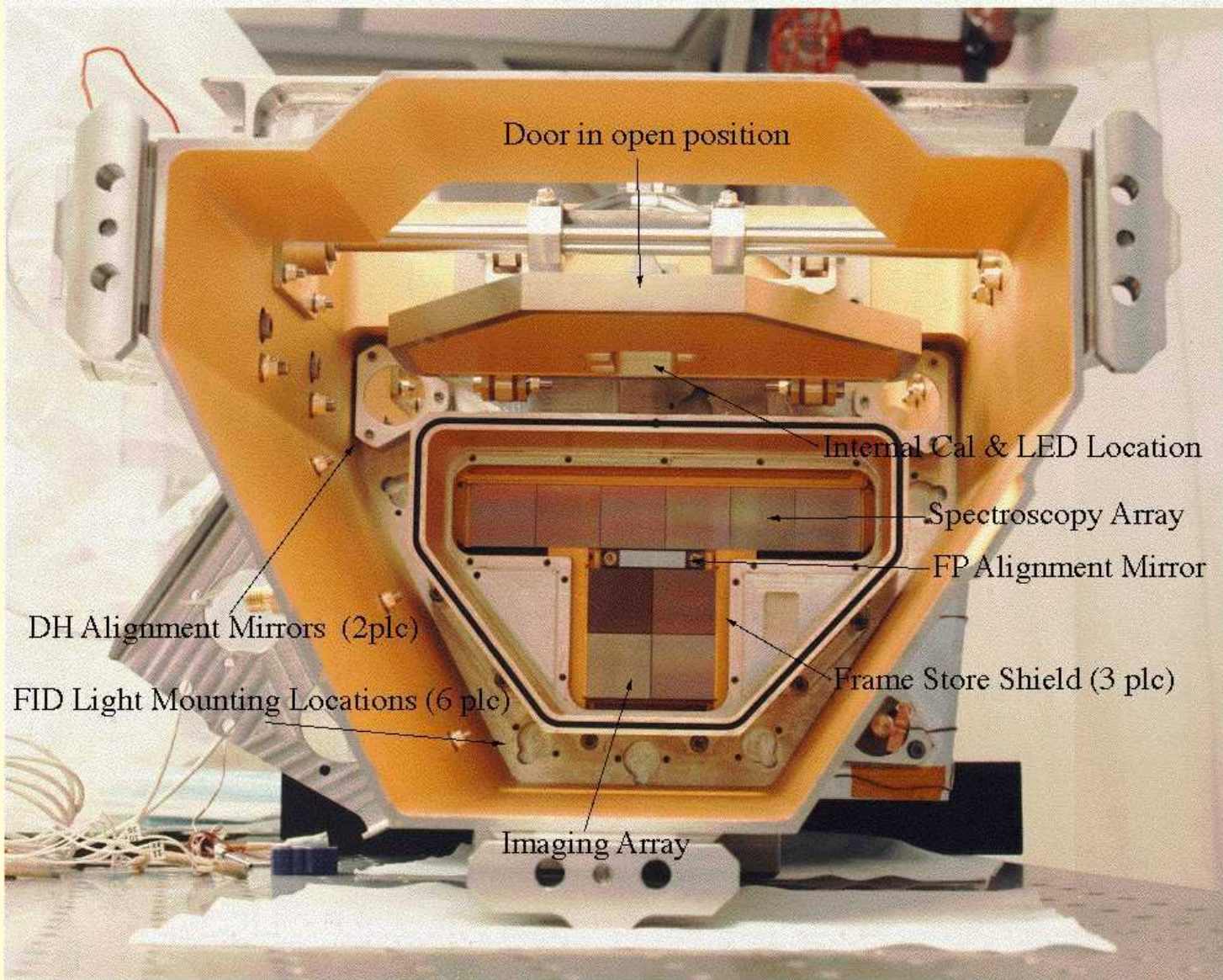


XMM-Newton (EPIC-MOS; Leicester): 7 single CCDs with 600×600 pixels, mounting is adapted to curved focal plane of the Wolter telescope.



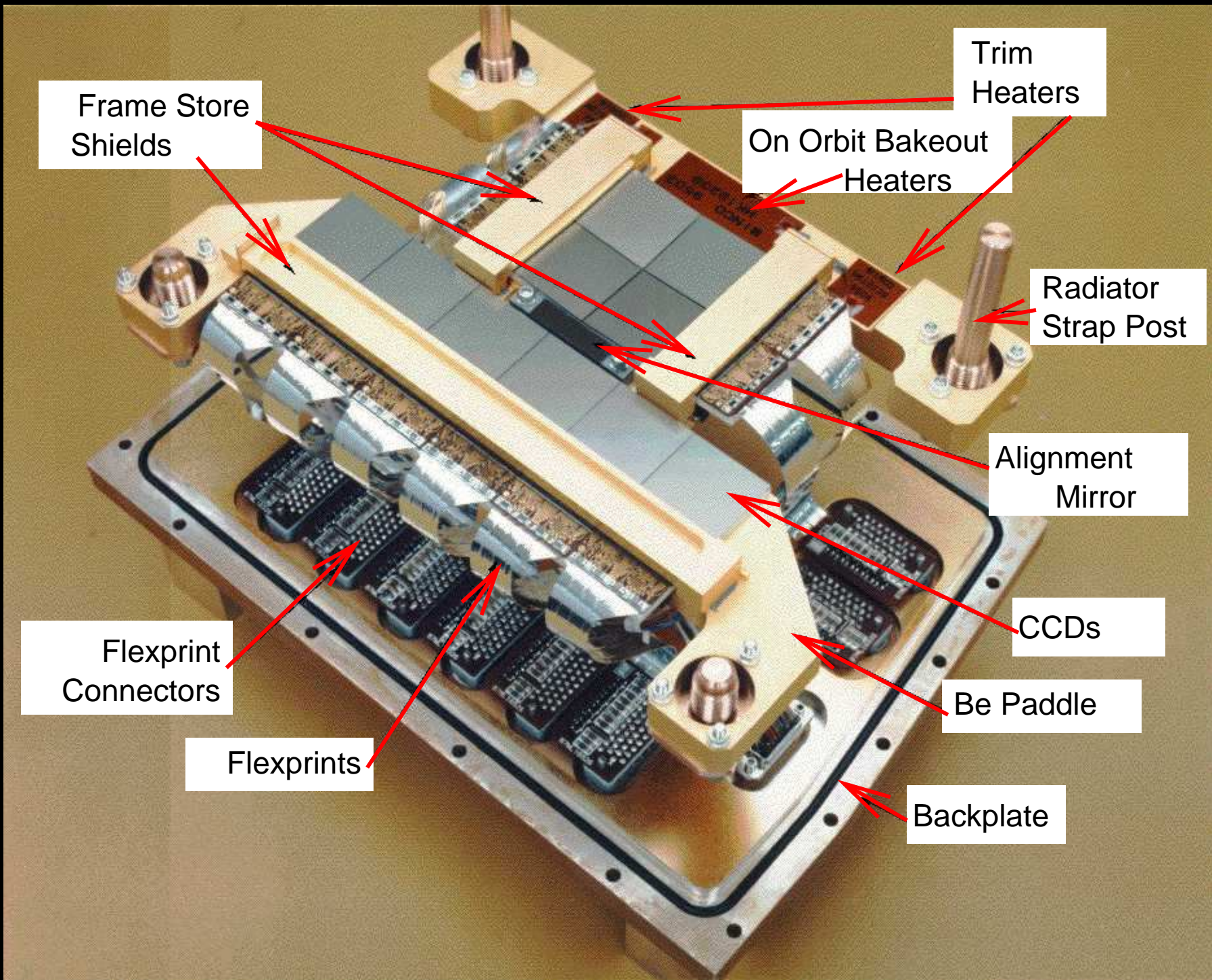
ESA

Chandra: ACIS



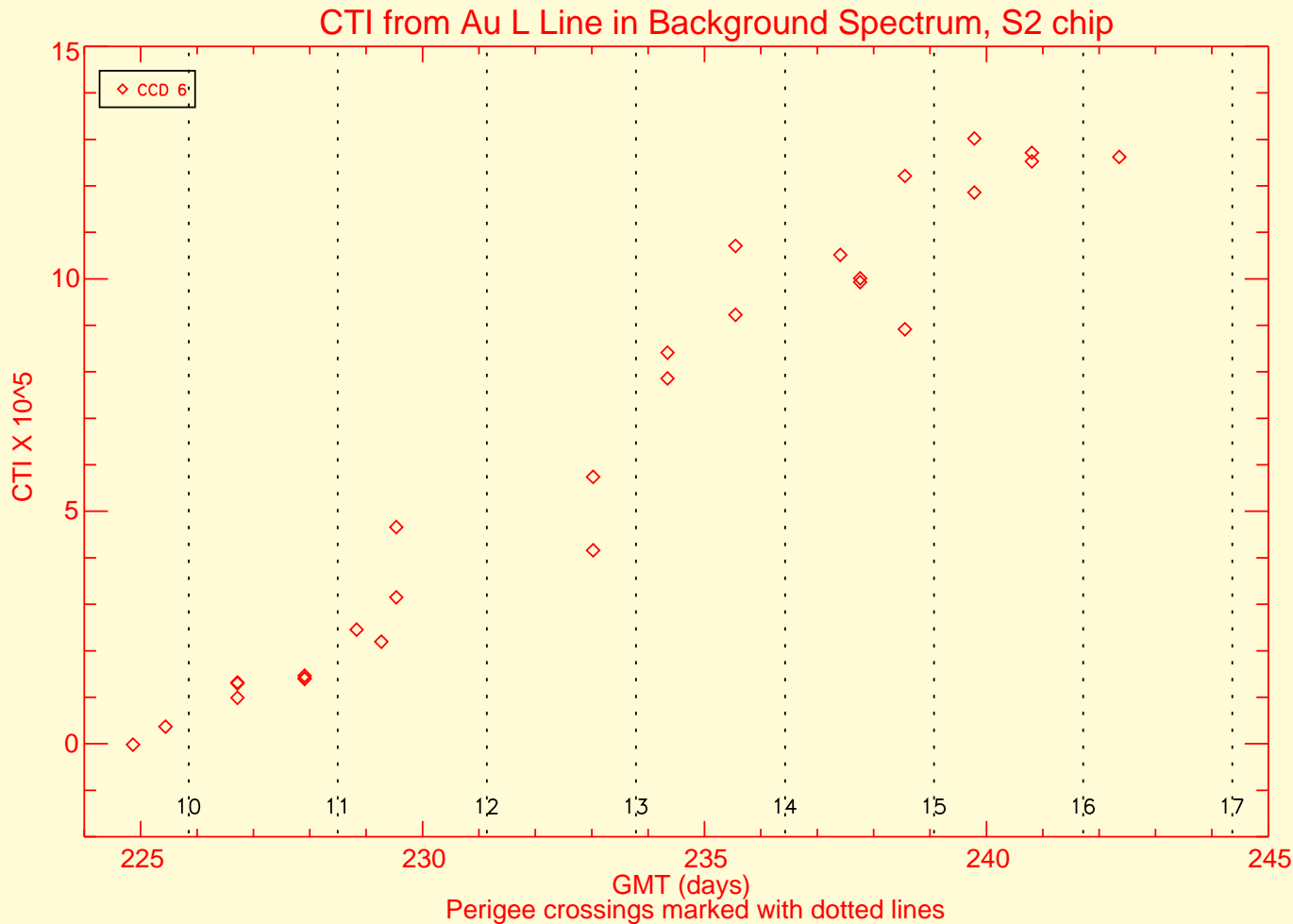
Chandra (ACIS):
10 **frame store**
CCDs

MIT-CXC



after MIT-CXC

Chandra: ACIS

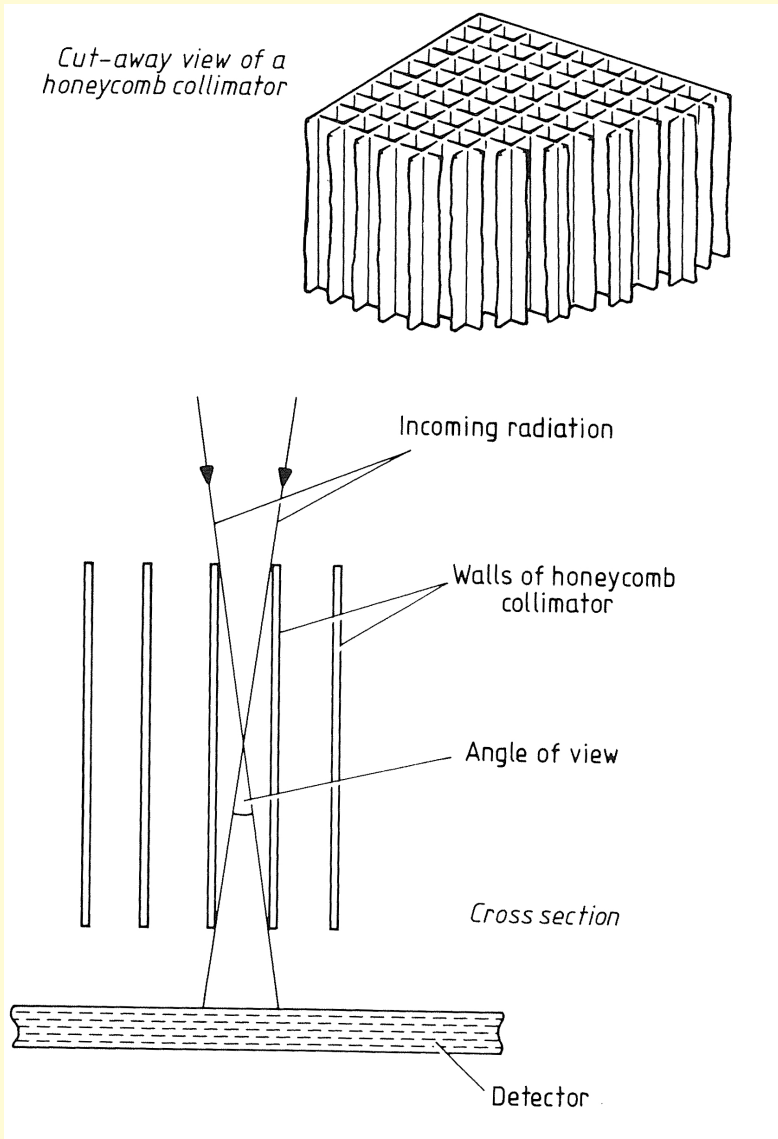


Shortly after launch in 1999 July, ACIS front illuminated CCDs showed significant increase in Charge Transfer Inefficiency (CTI).

Explanation: Low energy protons ($E < 1$ MeV) damaging gate structure of FI chips; are focused onto CCD by mirrors.

CTI: Fraction of charge lost when transporting electrons from one pixel to the next. Often also used: Charge Transfer Efficiency (CTE) ($CTE = 1 - CTI$).

Collimators



At energies above ~ 10 keV, imaging with mirror systems is not technically possible.

Apart from multilayer-technologies, but those have not yet flown.

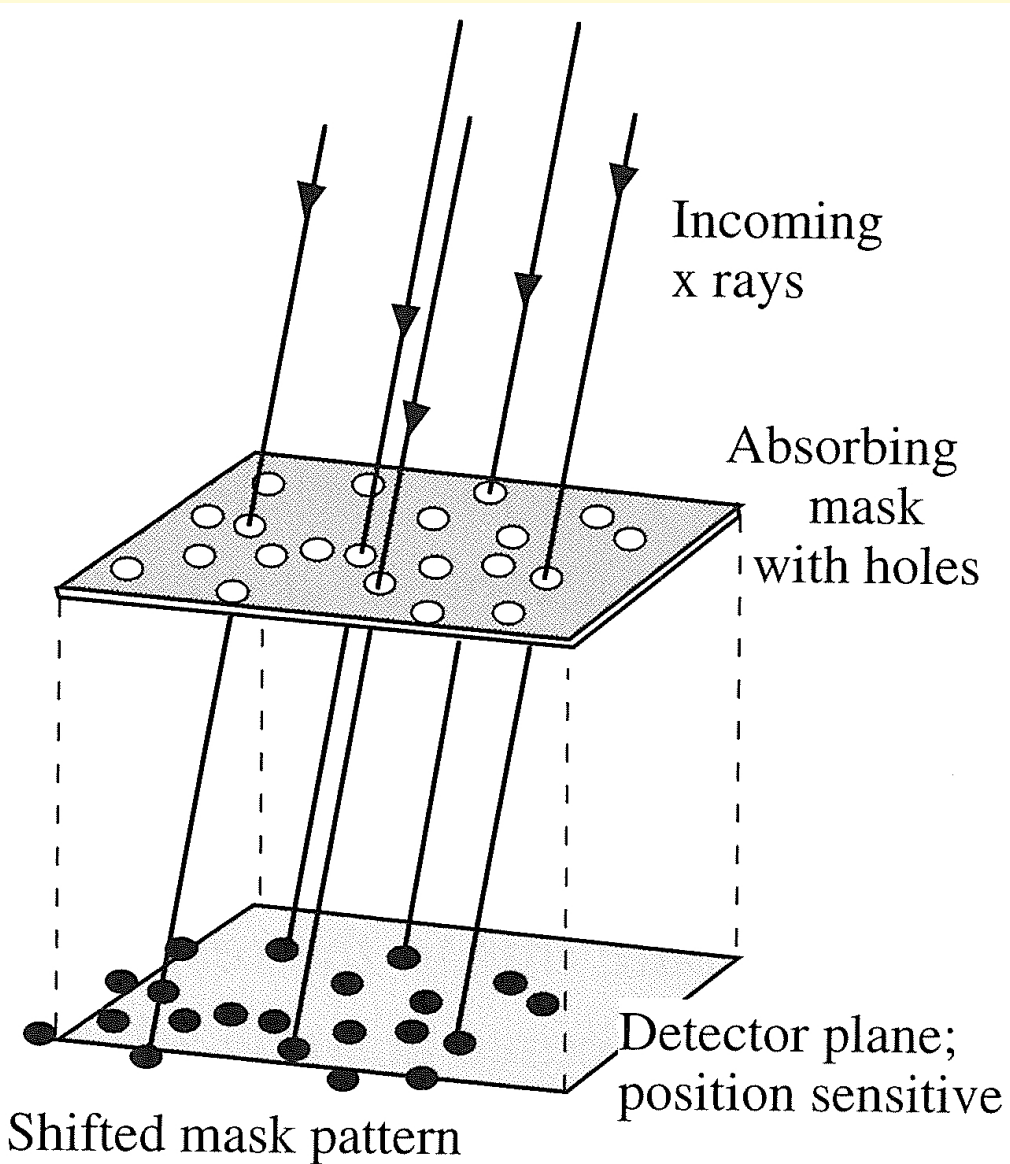
⇒ need other ways to ensure that we only see the object we want to see.

Simplest method: **honeycomb collimator**, i.e., a variant of a **pinhole camera**.

Field of view: $FOV \sim d/h$ where d tube diameter, h tube length; typical values \sim degrees.

(Kitchin, Astrophysical Techniques, Fig. 1.3.5)

Coded Mask Telescopes



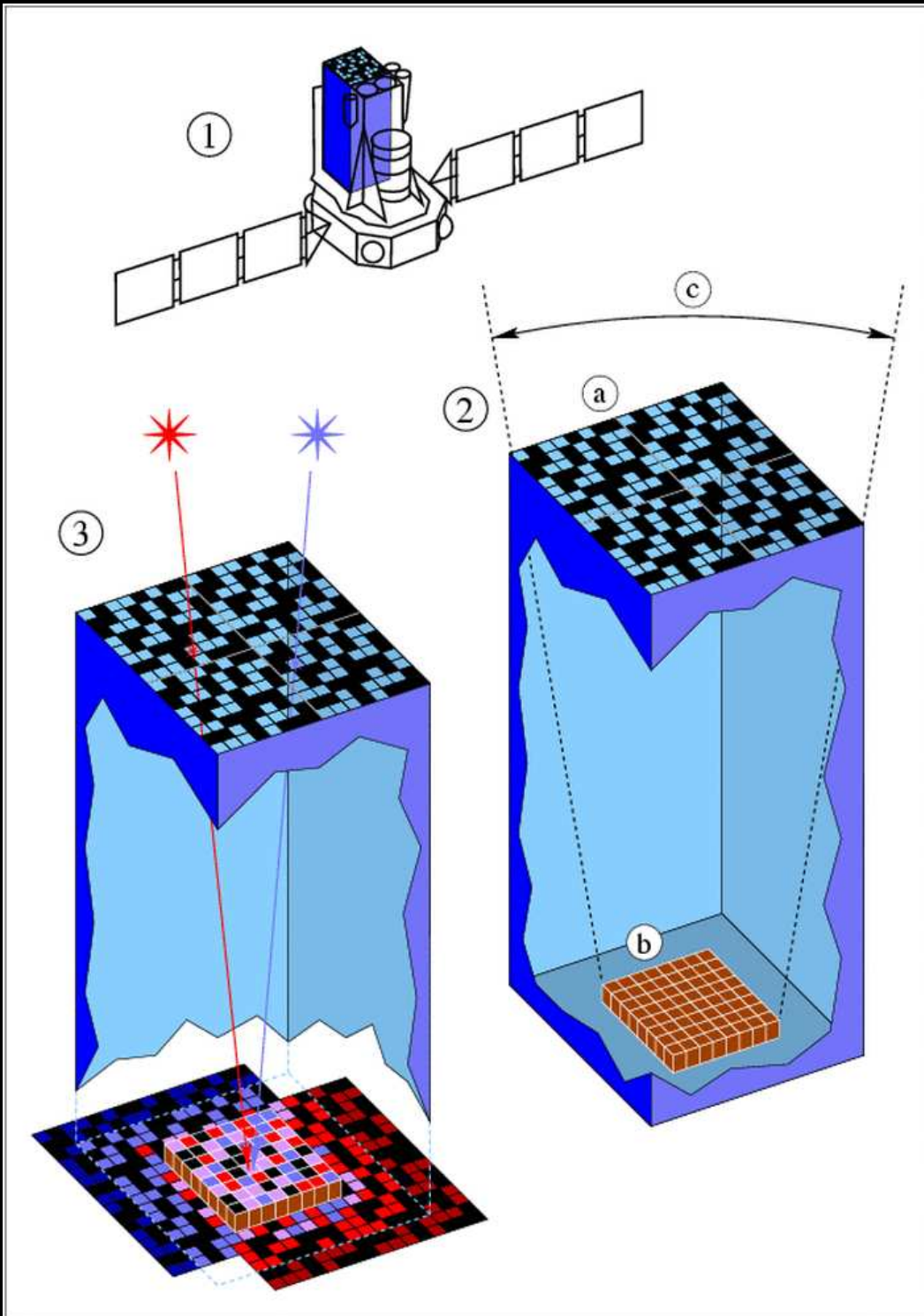
Problem of collimators: no imaging capabilities

Solution: Coded Masks

⇒ Combination of mask with multiple holes and position sensitive detector.

Typically, 25% to 50% of the mask is open.

(Bradt, Fig. 5.3)



Principle of image reconstruction:
correlate mask image with detector
plane image.

Define the "Response" of pixel x, y via

$$R(x, y) = C(x, y) - \langle C \rangle \quad (18)$$

where $C(x, y)$: measured count rate in
detector plane, and $\langle C \rangle$ mean count rate of
detector plane.

Compare $R(x, y)$ to response expected if there
were a source at position α, δ on the sky using
a cross correlation function

$$\text{CCF}(\alpha, \delta) = \iint_{\forall x, y} R(x, y) R(\alpha, \delta; x, y) dx dy \quad (19)$$

CCF has peak if good match with real source
found.

Then subtract off this source and repeat
("IROS"-method, "Iterative Removal of
Sources")

Imaging and spectral above 20 keV, entering the Gamma-ray domain

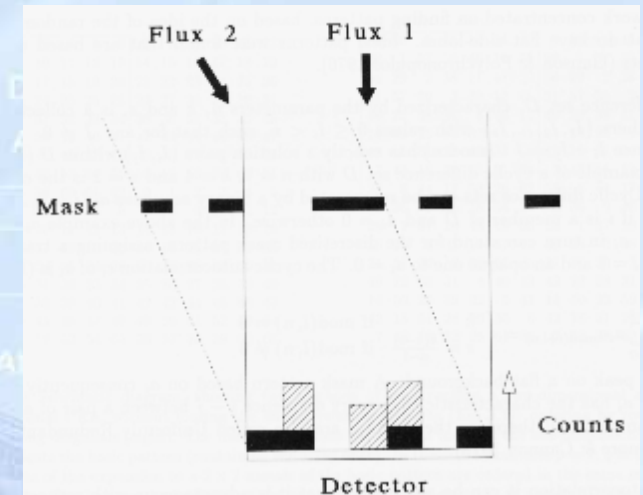
BIS coded mask

Coded-mask imaging



The combined shadow of several sources through a specifically designed mask can be used to determine the directions of each source.

Instrument computers and electronics



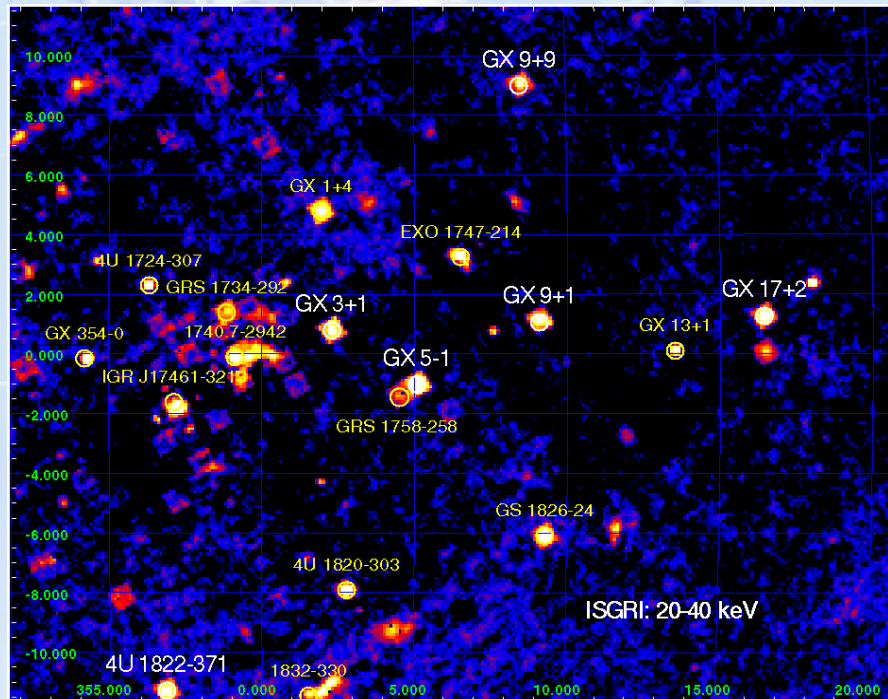
Power regulation

SWIFT

coded-mask

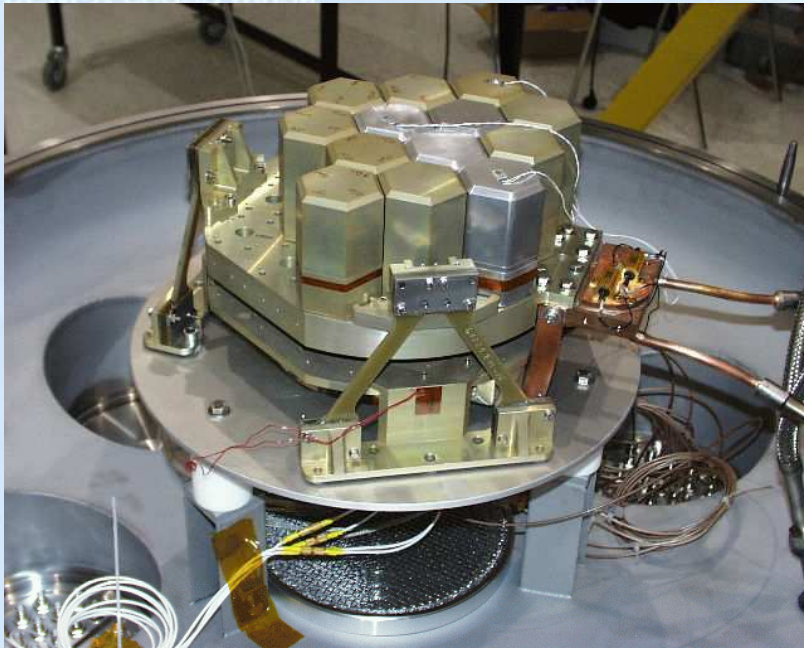
algorithms for pointing the spacecraft

Data handling and telecommunication



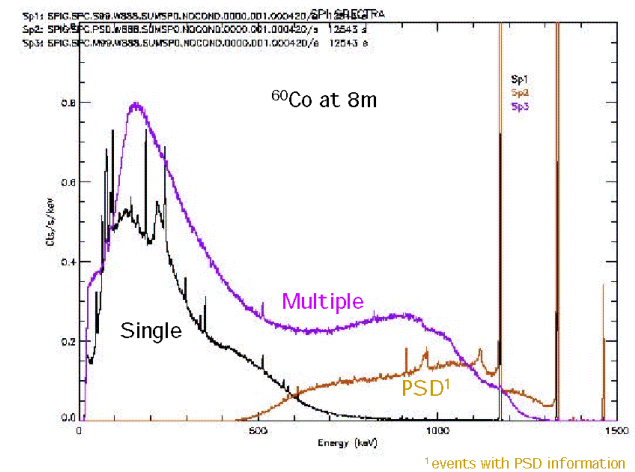
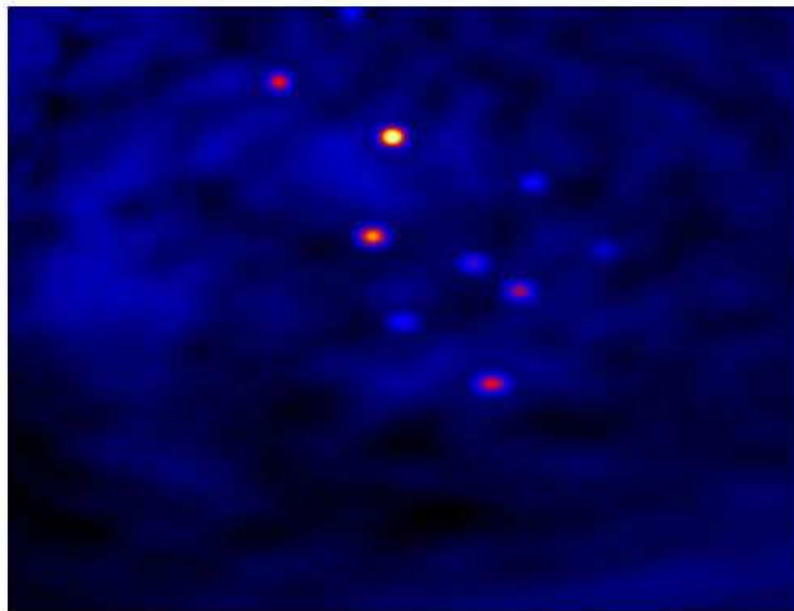
Coded mask image in hard X-rays (20-40 keV)

INTEGRAL – SPI, going up in energy to MeV (0.001 nm) range.



The coded mask.

Ge crystals
Same principle as room temp. but needs extreme cooling.

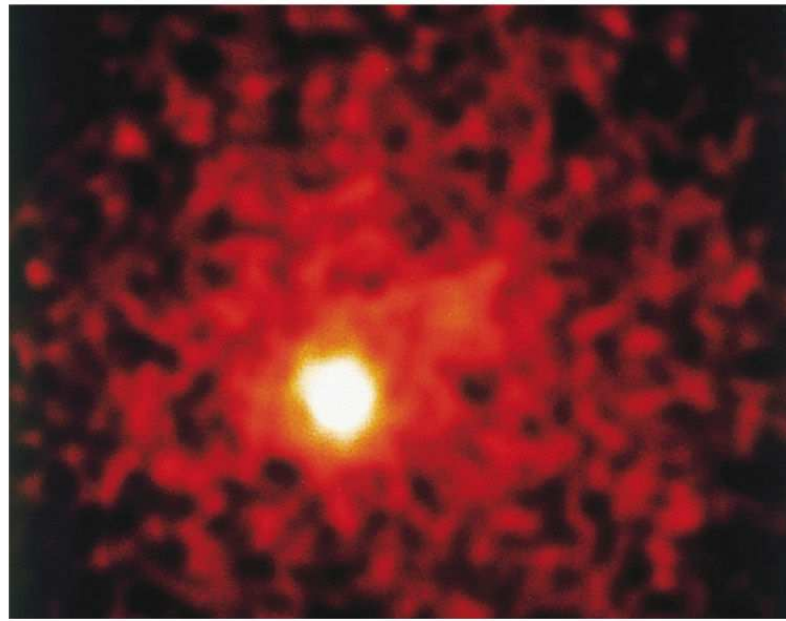


superb energy resolution

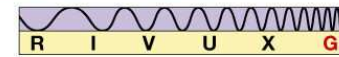
Gamma-ray instruments, Compton imaging



(a)



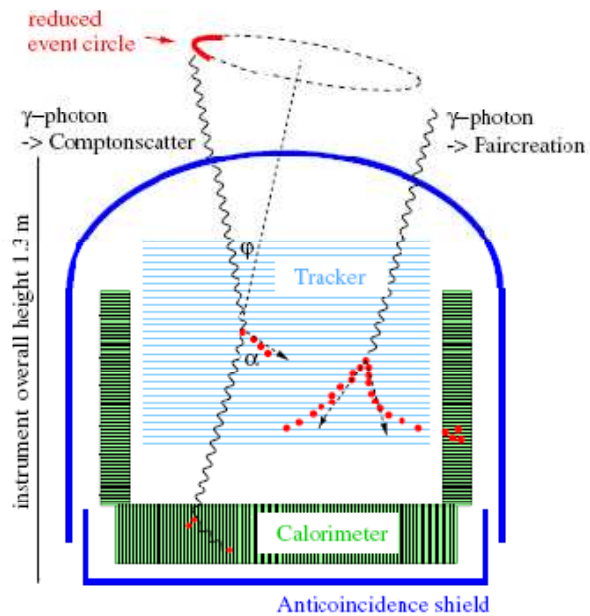
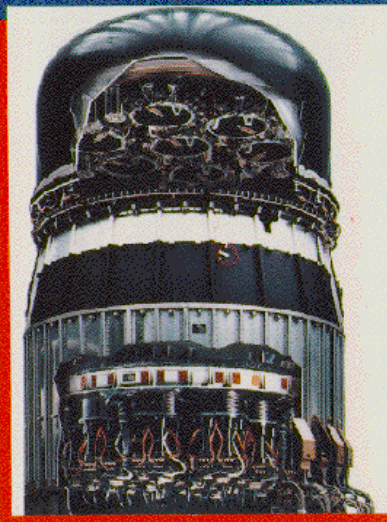
(b)



CGRO

Copyright © 2005 Pearson Prentice Hall, Inc.

Imaging Compton Telescope (COMPTEL)



MEGA